CHAPTER

15

Compressible Flow

OUTLINE

CHAPTER OBJECTIVES

- To introduce the fundamental compressible flow interactions between velocity, density, pressure, and temperature
- To describe the features of isentropic flows in ducts with smoothly varying cross-sectional area
- To derive the jump conditions across normal shock waves from the conservation equations
- To describe the effects of friction and heat transfer in compressible flows through constant-area ducts
- To indicate how wall geometry produces pressure waves that cause fluid compression, expansion, and turning in steady supersonic flows near walls

15.1. INTRODUCTION

Up to this point, this text has primarily covered incompressible flows. This chapter presents some of the elementary aspects of flows in which pressure-induced changes in density are important. The subject of compressible flow is also called *gas dynamics*, and it has wide applications in high-speed flows around objects of engineering interest. These include *external flows* such as those around projectiles, rockets, re-entry vehicles, and airplanes; and *internal flows* in ducts and passages such as nozzles and diffusers used in jet engines and rocket motors. Compressibility effects are also important in astrophysics. Recommended gas dynamics texts that further discuss the material presented here are Shapiro (1953), Liepmann and Roshko (1957), and Thompson (1972).

Several startling and fascinating phenomena arise in compressible flows (especially in the supersonic range) that defy expectations developed from incompressible flows. Discontinuities (shock waves) appear within the flow, and a rather strange circumstance arises in which an increase of flow area *accelerates* a supersonic stream. And, in subsonic compressible duct flow, friction can increase the flow's speed and heat addition can lower the flow's temperature. These phenomena, which have no counterparts in low-speed flows, are therefore worthy of our attention. Except for the treatment of friction in constant area ducts in Section 15.8, the material presented here is limited to that of frictionless flows outside boundary layers. In spite of this simplification, the results presented here have a great deal of practical value because boundary layers are especially thin in high-speed flows. Gravitational effects, which are of minor importance in high-speed flows, are also neglected.

As discussed in Section 4.11, the importance of compressibility in the equations of motion can be assessed by considering the Mach number M, defined as

$$M \equiv U/c, \tag{4.111}$$

where U is a representative flow speed, and c is the speed of sound, a thermodynamic quantity defined by:

$$c^2 \equiv (\partial p/\partial \rho)_s. \tag{1.19}$$

Here the subscript s signifies that the partial derivative is taken at constant entropy. In particular, the dimensionless scaling (4.109) of the compressible-flow continuity equation for isentropic conditions leads to:

$$\nabla \cdot u = -M^2 \left(\frac{\rho_0}{\rho}\right) \frac{D}{Dt}\left(\frac{p - p_0}{\rho_0 U^2}\right), \tag{4.110}$$

where ρ_0 and p_0 are appropriately chosen reference values for density and pressure. In (4.110), the pressure is scaled by fluid inertia parameters as is appropriate for primarily frictionless high-speed flow. In engineering practice, the incompressible flow assumption is presumed valid *if* $M < 0.3$, *but not at higher Mach numbers*. Equation (4.110) suggests that $M = 0.3$ corresponds to ~10% departure from perfectly incompressible flow behavior when the remainder of the right side of (4.110) is of order unity.

Although the significance of the ratio U/c was known for a long time, the Swiss aerodynamist Jacob Ackeret introduced the term *Mach number*, just as the term *Reynolds number*

was introduced by Sommerfeld many years after Reynolds' experiments. The name of the Austrian physicist Ernst Mach (1836–1916) was chosen because of his pioneering studies on supersonic motion and his invention of the so-called *Schlieren method* for optical visualization of flows involving density changes; see von Karman (1954, p. 106). (Mach distinguished himself equally well in philosophy. Einstein acknowledged that his own thoughts on relativity were influenced by "Mach's principle," which states that properties of space have no independent existence but are determined by the mass distribution within it. Strangely, Mach never accepted either the theory of relativity or the atomic structure of matter.)

Using the Mach number, compressible flows can be nominally classified as follows:

(i) *Incompressible flow*: $M = 0$. Fluid density does not vary with pressure in the flow field. The flowing fluid may be a compressible gas but its density may be regarded as constant.

(ii) *Subsonic flow*: $0 < M < 1$. The Mach number does not exceed unity anywhere in the flow field. Shock waves do not appear in the flow. In engineering practice, subsonic flows for which $M < 0.3$ are often treated as being incompressible.

(iii) *Transonic flow*: The Mach number in the flow lies in the range 0.8–1.2. Shock waves may appear. Analysis of transonic flows is difficult because the governing equations are inherently nonlinear, and also because a separation of the inviscid and viscous aspects of the flow is often impossible. (The word *transonic* was invented by von Karman and Hugh Dryden, although the latter argued in favor of spelling it *transsonic*. Von Karman [1954] stated, "I first introduced the term in a report to the U.S. Air Force. I am not sure whether the general who read the word knew what it meant, but his answer contained the word, so it seemed to be officially accepted" [p. 116].)

(iv) *Supersonic flow*: $M > 1$. Shock waves are generally present. In many ways analysis of a flow that is supersonic everywhere is easier than an analysis of a subsonic or incompressible flow as we shall see. This is because information propagates along certain directions, called *characteristics*, and a determination of these directions greatly facilitates the computation of the flow field.

(v) *Hypersonic flow*: $M > 3$. Very high flow speeds combined with friction or shock waves may lead to sufficiently large increases in a fluid's temperature that molecular dissociation and other chemical effects occur.

Perfect Gas Thermodynamic Relations

As density changes are accompanied by temperature changes, thermodynamic principles are constantly used throughout this chapter. Most of the necessary concepts and relations have been summarized in Sections 1.8 and 1.9, which may be reviewed before proceeding further. The most frequently used relations, valid for a perfect gas with constant specific heats, are listed here for quick reference:

$$\text{Internal energy } e = C_v T,$$

$$\text{Enthalpy } h = C_p T,$$

$$\textit{Thermal equation of state: } p = \rho RT,$$

$$\textit{Specific heats: } C_v = \frac{R}{\gamma - 1},\ C_p = \frac{\gamma R}{\gamma - 1},\ C_p - C_v = R, \quad \text{and} \quad \gamma = C_p/C_v, \tag{15.1}$$

$$\textit{Speed of sound: } c = \sqrt{\gamma RT} = \sqrt{\gamma p/\rho},$$

$$\textit{Entropy change: } S_2 - S_1 = C_p \ln\left(\frac{T_2}{T_1}\right) - R \ln\left(\frac{p_2}{p_1}\right) = C_v \ln\left(\frac{T_2}{T_1}\right) - R \ln\left(\frac{\rho_2}{\rho_1}\right).$$

An isentropic process of a perfect gas between states 1 and 2 obeys the following relations:

$$\frac{p_2}{p_1} = \left(\frac{\rho_2}{\rho_1}\right)^{\gamma}, \quad \text{and} \quad \frac{T_2}{T_1} = \left(\frac{\rho_2}{\rho_1}\right)^{\gamma-1} = \left(\frac{p_2}{p_1}\right)^{(\gamma-1)/\gamma}. \tag{15.2}$$

Some important properties of air at ordinary temperatures and pressures are:

$$R = 287\ \mathrm{m^2/(s^2\ K)},\ C_v = 717\ \mathrm{m^2/(s^2\ K)},\ C_p = 1004\ \mathrm{m^2/(s^2\ K)}, \quad \text{and} \quad \gamma = 1.40; \tag{15.3}$$

these values are useful for solution of the exercises at the end of this chapter.

15.2. ACOUSTICS

Perhaps the simplest and most common form of compressible flow is found when the pressure and velocity variations are small compared to steady reference values and the variations in pressure are isentropic. This branch of compressible flow is known as *acoustics* and is concerned with the study of sound waves. Acoustics is the linearized theory of compressible fluid dynamics and is a broad field with its own rich history (see Pierce, 1989). Our primary concern here is to deduce how the speed of sound enters the inviscid equations of fluid motion and to develop some insight into the behavior of pressure disturbances in compressible flow.

To determine the field equation governing acoustic phenomena, the dependent field variables may be separated into nominally steady and fluctuating values:

$$u_i = U_i + u_i',\ p = p_0 + p',\ \rho = \rho_0 + \rho', \quad \text{and} \quad T = T_0 + T', \tag{15.4}$$

where U_i, p_0, ρ_0, and T_0 are constants applicable to the region of interest, and all the fluctuating quantities—denoted by primes in (15.4)—are considered to be small compared to these. In addition, the isentropic condition allows the pressure to be Taylor expanded about the reference thermodynamic state specified by p_0 and ρ_0:

$$p = p_0 + p' = p_0 + \left(\frac{\partial p}{\partial \rho}\right)_s (\rho - \rho_0) + \frac{1}{2}\left(\frac{\partial^2 p}{\partial \rho^2}\right)_s (\rho - \rho_0)^2 + \ldots = p_0 + c^2\rho' + \frac{1}{2}\left(\frac{\partial^2 p}{\partial \rho^2}\right)_s \rho'^2 + \ldots$$

For small isentropic variations, the second-order and higher terms can be neglected, and this leads to a simple relationship between acoustic pressure and density fluctuations:

$$p' \cong c^2\rho', \tag{15.5}$$

where c^2 is given by (1.19). Using (15.2) and evaluating the derivative at the local reference values yields

$$c^2 = \gamma p_0/\rho_0 = \gamma R T_0, \tag{15.6}$$

where T_0 is the local reference temperature. Thus, we see that c is larger in monotonic and low-molecular weight gases (where γ and R are larger), and that it increases with increasing local temperature. Equation (15.5) is valid when the fractional density change or *condensation* $\equiv \rho'/\rho_0 = p'/\rho_0 c^2$ is much less than unity. Thus, the primary parametric requirement for the validity of acoustic theory is:

$$p'/\rho_0 c^2 \ll 1. \tag{15.7}$$

For ordinary sound levels in air, acoustic-pressure magnitudes are of order 1 Pa or less, so the ratio specified in (15.7) is typically less than 10^{-5} since $\rho_0 c^2 = \gamma p_0 \approx 1.4 \times 10^5$ Pa. Additionally, positive p' is called *compression* while negative p' is called *expansion* (or *rarefaction*). Acoustic pressure disturbances are commonly composed of equal amounts of compression and expansion.

The first approximate expression for c was found by Newton, who assumed that p'/p_0 was equal to ρ'/ρ_0 (Boyle's law) as would be true if the process undergone by a fluid particle was isothermal. In this manner Newton arrived at the expression $c = \sqrt{RT_0}$. He attributed the discrepancy of this formula with experimental measurements as due to "unclean air." However, the science of thermodynamics was virtually nonexistent at the time, so that the idea of an isentropic process was unknown to Newton. The correct expression for the sound speed was first given by Laplace.

The field equation for acoustic pressure disturbances is obtained from the continuity equation (4.7) and the Euler equation (4.41) with $\mathbf{g} = 0$, by linearizing these equations and then combining them to reach a single equation for p'. The linearization is accomplished by inserting (15.4) into (4.7) and (4.41) with $\mathbf{g} = 0$, and dropping the terms that include products of primed field variables:

$$\frac{\partial \rho}{\partial t} + \frac{\partial \rho u_j}{\partial x_j} = \frac{\partial(\rho_0 + \rho')}{\partial t} + \frac{\partial\left(\rho_0 U_j + \rho' U_j + \rho_0 u_j' + \rho' u_j'\right)}{\partial x_j} \cong \frac{\partial \rho'}{\partial t} + U_j \frac{\partial \rho'}{\partial x_j} + \rho_0 \frac{\partial u_j'}{\partial x_j} = 0, \tag{15.8}$$

$$\begin{aligned} \frac{\partial u_i}{\partial t} + u_j \frac{\partial u_i}{\partial x_j} + \frac{1}{\rho}\frac{\partial p}{\partial x_i} &= \frac{\partial(U_i + u_i')}{\partial t} + (U_j + u_j')\frac{\partial(U_i + u_i')}{\partial x_j} + \frac{1}{\rho_o + \rho'}\frac{\partial(P + p')}{\partial x_i} \\ &\cong \frac{\partial u_i'}{\partial t} + U_j \frac{\partial u_i'}{\partial x_j} + \frac{1}{\rho_o}\frac{\partial p'}{\partial x_i} = 0. \end{aligned} \tag{15.9}$$

The next steps involve using (15.6) to eliminate ρ' from (15.8), and mildly rewriting (15.8) and (15.9),

$$\frac{1}{c^2}\left(\frac{\partial}{\partial t} + U_j \frac{\partial}{\partial x_j}\right)p' + \rho_0 \left(\frac{\partial}{\partial x_j}\right)u_j' = 0 \quad \text{and} \quad \left(\frac{\partial}{\partial t} + U_j \frac{\partial}{\partial x_j}\right)u_i' + \frac{1}{\rho_o}\left(\frac{\partial}{\partial x_i}\right)p' = 0, \tag{15.10, 15.11}$$

to see that the differentiation operations in the two equations are identical but act on different field variables. In this case cross-differentiation can be used to eliminate u_i'. Applying

$(\partial/\partial t + U_j\partial/\partial x_j)$ to (15.10) and $-\rho_0\partial/\partial x_j$ to (15.11) and adding the resulting equations leads to:

$$\frac{1}{c^2}\left(\frac{\partial}{\partial t} + U_j\frac{\partial}{\partial x_j}\right)^2 p' - \frac{\partial^2 p'}{\partial x_j \partial x_j} = 0, \tag{15.12}$$

which is the field equation for acoustic pressure disturbances in a uniform flow.

To highlight the importance of the sound speed, consider one-dimensional pressure disturbances $p'(x,t)$ that only vary along the x-axis in a stationary fluid ($U_j = 0$). For this case, the simplified forms of (15.12) and (15.11) are:

$$\frac{1}{c^2}\frac{\partial^2 p'}{\partial t^2} - \frac{\partial^2 p'}{\partial x^2} = 0, \quad \text{and} \quad u_1'(x,t) = -\frac{1}{\rho_o}\int \frac{\partial p'}{\partial x} dt, \tag{15.13, 15.14}$$

where (15.11) has been integrated to show how u_1' and p' are related. Equation (15.13) is the one-dimensional wave equation, and its solutions are of the form:

$$p'(x,t) = f(x - ct) + g(x + ct), \tag{15.15}$$

where f and g are functions determined by initial conditions (see Exercise 15.1). Equation (15.15) is known as *d'Alembert's solution*, and $f(x - ct)$ and $g(x + ct)$ represent traveling pressure disturbances that propagate to the right and left, respectively, with increasing time. Consider a pressure pulse $p'(x,t)$ that propagates to the right and is centered at $x = 0$ with shape $f(x)$ at $t = 0$ as shown in Figure 15.1. An arbitrary time t later, the wave is centered at $x = ct$ and its shape is described by $f(x - ct)$. Similarly, when $p'(x,t) = g(x + ct)$, the pressure disturbance propagates to the left and is located at $x = -ct$ at time t. Thus, the speed at which acoustic pressure disturbances travel is c, and this is independent of the shape of the pressure disturbance waveform.

However, the disturbance waveform does influence the fluid velocity u_1'. It can be determined from (15.14) and (15.15), and is given by

$$u_1'(x,t) = \frac{1}{\rho_o c}(f(x - ct) - g(x + ct)) \tag{15.16}$$

(see Exercise 15.2). Thus, the fluid velocity includes rightward- and leftward-propagating components that are matched to the pressure disturbance. Moreover, (15.16) shows that

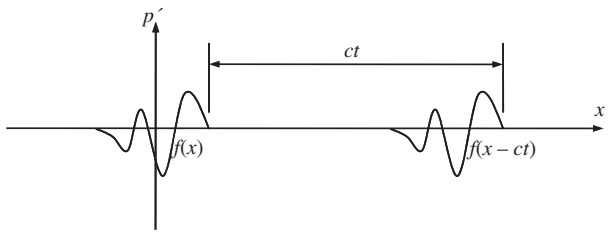

FIGURE 15.1 Propagation of an acoustic pressure disturbance p' that travels to the right with increasing time. At $t = 0$ the disturbance is centered at $x = 0$ and has waveform $f(x)$. At time t later, the disturbance has moved a distance ct but its waveform shape has not changed.

the compression portions of f and g lead to fluid velocity in the same direction as wave propagation; the fluid velocity from $f(x - ct)$ is to the right when $f > 0$, and the fluid velocity from $g(x + ct)$ is to the left when $g > 0$. Similarly, the expansion portions of f and g lead to fluid velocity in the direction opposite of wave propagation; the fluid velocity from $f(x - ct)$ is to the left when $f < 0$, and the fluid velocity from $g(x + ct)$ is to the right when $g < 0$. These fluid velocity directions are worth noting because they persist with the same signs when the wave amplitudes exceed those allowed by the approximation (15.7).

Now consider one-dimensional pressure waves $p'(x, t)$ when $U_j = (U, 0, 0)$ so that (15.12) becomes

$$\frac{1}{c^2}\left(\frac{\partial}{\partial t} + U\frac{\partial}{\partial x}\right)^2 p' - \frac{\partial^2 p'}{\partial x^2} = 0.$$

The general solution of this equation is:

$$p'(x, t) = f(x - (c + U)t) + g(x + (c - U)t). \tag{15.17}$$

When $U > 0$, the travel speed of the downstream-propagating waves is enhanced and that of the upstream-propagating waves is reduced. However, when the flow is supersonic, $U > c$, both portions of (15.17) travel downstream, and this represents a major change in the character of the flow. In subsonic flow, both upstream and downstream pressure disturbances may influence the flow at the location of interest, while in supersonic flow only upstream disturbances may influence the flow. For aircraft moving through a nominally quiescent atmosphere, this means that a ground-based observer below the aircraft's flight path may hear a subsonic aircraft before it is overhead. However, a supersonic aircraft does not radiate sound forward in the direction of flight so the same ground-based observer will only hear a supersonic aircraft after it has passed overhead (see Section 15.9).

Linear acoustic theory is valuable and effective for weak pressure disturbances, but it also indicates how nonlinear phenomena arise as pressure-disturbance amplitudes increase. The speed of sound in gases depends on the local temperature, $c = \sqrt{\gamma RT}$. For air at 15°C, this gives $c = 340$ m/s. The nonlinear terms that were dropped in the linearization (15.8) and (15.9) may change the waveform of a propagating nonlinear pressure disturbance depending on whether it is a compression or expansion. Because $\gamma > 1$, the isentropic relations show that if $p' > 0$ (compression), then $T' > 0$ so the sound speed c increases within a compression disturbance. Therefore, pressure variations within a region of nonlinear compression travel faster than a zero-crossing of p' where $c = \sqrt{\gamma RT_0}$ and therefore may catch up with the leading edge of the compressed region. Such compression-induced changes in c cause nonlinear compression waves to spontaneously steepen as they travel. The opposite is true for nonlinear expansion waves where $p' < 0$ and $T' < 0$, so c decreases. Here, any pressure variations within the region of expansion fall farther behind the leading edge of the expansion. This causes nonlinear expansion waves to spontaneously flatten as they travel. When combined these effects cause a nonlinear sinusoidal pressure disturbance involving equal amounts of compression and expansion to evolve into a saw-tooth shape (see Chapter 11 in Pierce, 1989). Pressure disturbances that do not satisfy the approximation (15.7) are called *finite* amplitude waves.

The limiting form of a finite-amplitude compression wave is a discontinuous change of pressure, commonly known as a *shock wave*. In Section 15.6 it will be shown that

finite-amplitude compression waves are not isentropic and that they propagate through a still fluid *faster* than acoustic waves.

15.3. BASIC EQUATIONS FOR ONE-DIMENSIONAL FLOW

This section presents fundamental results for steady compressible flows that can be analyzed using one spatial dimension. The specific emphasis here is on flow through a duct whose centerline may be treated as being straight and whose cross section varies slowly enough so that all dependent flow-field variables (u, p, ρ, T) are well approximated at any location as being equal to their cross-section-averaged values. If the duct area $A(x)$ varies with the distance x along the duct, as shown in Figure 15.2, the dependent flow-field variables are taken as $u(x)$, $p(x)$, $\rho(x)$, and $T(x)$. Unsteadiness (and much complexity) can be introduced by including t as an additional independent variable.

In this situation a control volume development of the basic equations is appropriate. Start with scalar equations representing conservation of mass and energy using the stationary control volume shown in Figure 15.2. For steady flow within this control volume, the integral form of the continuity equation (4.5) requires:

$$\rho_1 u_1 A_1 = \rho_2 u_2 A_2, \quad \text{or} \quad \rho u A = \dot{m} = const., \tag{15.18}$$

where $\dot{m}$ is the mass flow rate in the duct, and the second form follows from the first because the locations 1 and 2 are arbitrary. Forming a general differential of the second form and dividing the result by $\dot{m}$ produces:

$$\frac{d\rho}{\rho} + \frac{du}{u} + \frac{dA}{A} = 0. \tag{15.19}$$

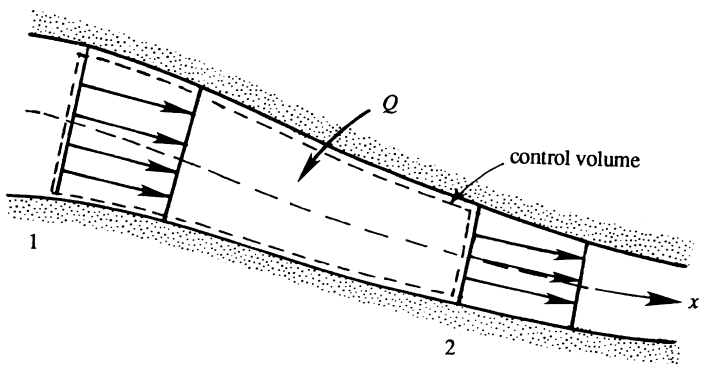

FIGURE 15.2 One-dimensional compressible flow in a duct with smoothly varying centerline direction and cross-sectional area. A stationary control volume in this duct is indicated by dotted lines. Conditions at the upstream and downstream control surfaces are denoted by "1" and "2," respectively. In some circumstances, heat Q may be added to the fluid in the volume. When the control surfaces normal to the flow are only a differential distance apart, then $x_2 = x_1 + dx$, $A_2 = A_1 + dA$, $u_2 = u_1 + du$, $p_2 = p_1 + dp$, $\rho_2 = \rho_1 + d\rho$, etc., where x is the duct's centerline coordinate, A is the duct's cross-sectional area, and u, p, and ρ are the cross-section averaged flow speed, pressure, and density.

For steady flow in a stationary control volume, the integral form of the energy equation (4.48) simplifies to:

$$\int_{A*} \rho\left(e+\frac{1}{2}u_i^2\right)u_j n_j dA = \int_{A*} u_i \tau_{ij} n_j dA - \int_{A*} q_j n_j dA, \tag{15.20}$$

where e is the internal energy per unit mass, A^* is the control surface, n_j is the outward normal on the control surface, the body force has been neglected, τ_{ij} is the stress tensor, and q_j is heat flux vector. The term on the left side represents the net flux of internal and kinetic energy out of the control volume. The first term on the right side represents the rate of work done on the control surface, and the second term on the right-hand side represents the heat *input* through the control surface. Here the minus sign in front of the final term occurs because $q_j n_j$ is positive when heat leaves the control volume. A term-by-term evaluation of (15.20) with the chosen control volume produces:

$$-\left(e+\frac{1}{2}u^2\right)_1 \dot{m} + \left(e+\frac{1}{2}u^2\right)_2 \dot{m} = (upA)_1 - (upA)_2 + \dot{m}Q, \tag{15.21}$$

where $\dot{m} = \rho_1 u_1 A_1 = \rho_2 u_2 A_2$ has been used, and Q is the heat added per unit mass of flowing fluid so that:

$$-\int_{A*} q_j n_j dA = \dot{m}Q.$$

Here the wall shear stress does no work, because $u_i = 0$ in (15.20) at the wall. Thus the surface work done on the control volume comes from the pressure on the control surfaces lying perpendicular to the flow direction. Dividing (15.21) by $\dot{m}$ and noting that $upA/\dot{m} = p/\rho$ allows it to be simplified to:

$$\left(e+\frac{p}{\rho}+\frac{1}{2}u^2\right)_2 - \left(e+\frac{p}{\rho}+\frac{1}{2}u^2\right)_1 = Q, \quad \text{or} \quad h_2+\frac{1}{2}u_2^2 - h_1 - \frac{1}{2}u_1^2 = Q, \tag{15.22}$$

where $h = e + p/\rho$, is the enthalpy per unit mass. This energy equation is valid even if there are frictional or nonequilibrium conditions (e.g., shock waves) between sections 1 and 2. It implies that the *sum of enthalpy and kinetic energy remains constant in an adiabatic flow.* Therefore, enthalpy plays the same role in a flowing system that internal energy plays in a nonflowing system. The difference between the two types of systems is the *flow work* required to push matter along the duct.

Now consider momentum conservation without the body force using the same control volume. The simplified version of (4.17) is:

$$\int_{A*} \rho u_i u_j n_j \, dA = \int_{A*} \tau_{ij} n_j \, dA. \tag{15.23}$$

The term on the left side represents the net flux of momentum out of the control volume and the term on the right side represents forces on the control surface. When applied to the control volume in Figure 15.2 for the x-direction, (15.23) becomes

$$-\dot{m}u_1 + \dot{m}u_2 = (pA)_1 - (pA)_2 + F, \tag{15.24}$$

where F is the x-component of the force exerted on the fluid in the control volume by the walls of the duct between locations 1 and 2. When the control volume has differential length, $x_2 = x_1 + dx$, then (15.24) can be written:

$$\dot{m}\frac{du}{dx} = -\frac{d}{dx}(pA) + p\frac{dA}{dx} - F_f = -A\frac{dp}{dx} - F_f, \tag{15.25}$$

where F_f is the perimeter friction force per unit length along the duct, and the second term in the middle portion of (15.25) is the pressure force on the control volume that occurs when the duct walls expand or contract. This term also appears in the derivation of (4.19), the inviscid steady-flow constant-density Bernoulli equation. For inviscid flow, F_f is zero and (15.25) simplifies to

$$\rho u A\frac{du}{dx} = -A\frac{dp}{dx}, \quad \text{or} \quad udu + \frac{dp}{\rho} = 0, \tag{15.26}$$

where $\dot{m}$ in (15.25) has been replaced by $\rho u A$. The second equation of (15.26) is the Euler equation without a body force. A frictionless and adiabatic flow is isentropic, so the property relation (1.18) implies:

$$TdS = dh - dp/\rho = 0, \quad \text{so } dh = dp/\rho.$$

Inserting the last relationship into the second equation of (15.26) and integrating produces:

$$h + \frac{1}{2}u^2 = const.$$

This is the steady Bernoulli equation for isentropic compressible flow (4.78) without the body force term. It is identical to (15.22) when $Q = 0$.

To summarize, the equations for steady one-dimensional compressible flow in a duct with slowly varying area are (15.19), (15.22), and (15.25).

15.4. REFERENCE PROPERTIES IN COMPRESSIBLE FLOW

In incompressible flows, boundary conditions or known properties or profiles typically provide reference values for h, c, T, p, and ρ. In compressible flows, these thermodynamic variables depend on the flow's speed. Thus, reference values for thermodynamic variables must include a specification of the flow speed. The most common reference conditions are the stagnation state ($u = 0$) and the sonic condition ($u = c$), and these are discussed in turn in this section.

If the properties of a compressible flow (h, ρ, u, etc.) are known at a certain point, the reference stagnation properties at that point are defined as those that would be obtained if the local flow were *imagined* to slow down to zero velocity *isentropically*. Stagnation properties are denoted by a subscript zero in gas dynamics. Thus the *stagnation enthalpy* is defined as

$$h_0 \equiv h + \frac{1}{2}u^2.$$

For a perfect gas, this implies

$$C_p T_0 = C_p T + \frac{1}{2}u^2, \tag{15.27}$$

which defines the *stagnation temperature*. Ratios of local and stagnation variables are often sought, and these can be expressed in terms of the Mach number, M. For example (15.27) can be rearranged to find:

$$\frac{T_0}{T} = 1 + \frac{u^2}{2C_p T} = 1 + \frac{\gamma - 1}{2}\frac{u^2}{\gamma RT} = 1 + \frac{\gamma - 1}{2}M^2, \tag{15.28}$$

where $C_p = \gamma R/(\gamma - 1)$ from (15.1) has been used. Thus the stagnation temperature T_0 can be found for a given T and M. The isentropic relations (15.2) can then be used to obtain the *stagnation pressure* and *stagnation density*:

$$\frac{p_0}{p} = \left(\frac{T_0}{T}\right)^{\gamma/(\gamma-1)} = \left[1 + \frac{\gamma - 1}{2}M^2\right]^{\gamma/(\gamma-1)}, \quad \text{and}$$
$$\frac{\rho_0}{\rho} = \left(\frac{T_0}{T}\right)^{1/(\gamma-1)} = \left[1 + \frac{\gamma - 1}{2}M^2\right]^{1/(\gamma-1)}. \tag{15.29, 15.30}$$

In a general flow the stagnation properties can vary throughout the flow field. If, however, the flow is adiabatic (but not necessarily isentropic), then $h + u^2/2$ is constant throughout the flow as shown by (15.22). It follows that h_0, T_0, *and* c_0 $(= \sqrt{\gamma RT_0})$ *are constant throughout an adiabatic flow, even in the presence of friction. In contrast, the stagnation pressure* p_0 *and density* ρ_0 *decrease if there is friction*. To see this, consider the entropy change in an adiabatic flow between sections 1 and 2 in a smoothly varying duct, with 2 being the downstream section. Let the flow at both sections hypothetically be brought to rest by isentropic processes, giving the local stagnation conditions p_{01}, p_{02}, T_{01}, and T_{02}. Then the entropy change between the two sections can be expressed as

$$S_2 - S_1 = S_{02} - S_{01} = -R \ln \frac{p_{02}}{p_{01}} + C_p \ln \frac{T_{02}}{T_{01}},$$

from the final equation of (15.1). The last term is zero for an adiabatic flow in which $T_{02} = T_{01}$. As the second law of thermodynamics requires that $S_2 > S_1$, it follows that

$$p_{02} < p_{01},$$

which shows that the stagnation pressure falls due to friction. And, from $p_0 = \rho_0 RT_0$, ρ_0 must fall too for constant T_0.

It is apparent that all stagnation properties are constant along an isentropic flow. If such a flow happens to start from a large reservoir where the fluid is practically at rest, then the properties in the reservoir equal the stagnation properties everywhere in the flow (Figure 15.3).

In addition to the stagnation properties, there is another useful set of reference quantities. These are called *sonic* or *critical* conditions and are commonly denoted by an asterisk. Thus, p^*, ρ^*, c^*, and T^* are properties attained if the local fluid is imagined to expand or compress

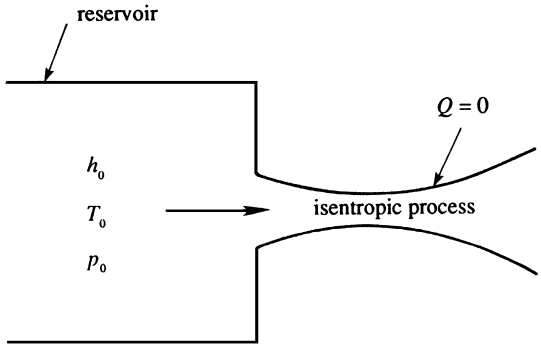

FIGURE 15.3 Schematic of an isentropic compressible-flow process starting from a reservoir. An isentropic process is both adiabatic (no heat exchange) and frictionless. Stagnation properties, indicated with a subscript 0, are uniform everywhere and are equal to the properties in the reservoir.

isentropically until it reaches $M = 1$. The sonic area A^* is often the most useful or important because the stagnation area is infinite for any compressible duct flow. If M is known where the duct area is A, the passage area, A^*, at which the sonic conditions are attained can be determined to be

$$\frac{A}{A^*} = \frac{1}{M}\left[\frac{2}{\gamma+1}\left(1+\frac{\gamma-1}{2}M^2\right)\right]^{(1/2)(\gamma+1)/(\gamma-1)} \tag{15.31}$$

(see Exercise 15.4).

We shall see in the following section that sonic conditions can only be reached at the *throat* of a duct, where the area is minimum. However, a throat need not actually exist in the flow; the sonic variables are simply reference values that are reached *if* the flow were brought to the sonic state isentropically. From its definition it is clear that the value of A^* in a flow remains constant in isentropic flow. The presence of shock waves, friction, or heat transfer changes the value of A^* along the flow.

The values of T_0/T, P_0/P, ρ_0/ρ, and A/A^* at a point can be determined from (15.28) through (15.31) if the local Mach number is known. For $\gamma = 1.4$, these ratios are tabulated in Table 15.1. The reader should examine this table at this point. Examples 15.1 and 15.2 illustrate the use of this table.

15.5. AREA-VELOCITY RELATIONSHIP IN ONE-DIMENSIONAL ISENTROPIC FLOW

Some surprising consequences of compressibility are found in isentropic flow through a duct of varying area. The natural application area for this topic is in the design of *nozzles* and *diffusers*. A nozzle is a device through which the flow expands from high to low pressure to generate a high-speed jet. Examples of nozzles are the exit ducts of a fireman's hose or a rocket motor. A diffuser's function is opposite that of a nozzle (and it has little or nothing to do with the diffusive transport of heat or species by molecular motion). In a diffuser

TABLE 15.1 Isentropic Flow of a Perfect Gas ($\gamma = 1.4$)

M	p/p_0	ρ/ρ_0	T/T_0	$A/A*$	M	p/p_0	ρ/ρ_0	T/T_0	$A/A*$
0	1	1	1	∞	0.62	0.7716	0.8310	0.9286	1.1656
0.02	0.9997	0.9998	0.9999	28.9421	0.64	0.7591	0.8213	0.9243	1.1451
0.04	0.9989	0.9992	0.9997	14.4815	0.66	0.7465	0.8115	0.9199	1.1265
0.06	0.9975	0.9982	0.9993	9.6659	0.68	0.7338	0.8016	0.9153	1.1097
0.08	0.9955	0.9968	0.9987	7.2616	0.7	0.7209	0.7916	0.9107	1.0944
0.1	0.9930	0.9950	0.9980	5.8218	0.72	0.7080	0.7814	0.9061	1.0806
0.12	0.9900	0.9928	0.9971	4.8643	0.74	0.6951	0.7712	0.9013	1.0681
0.14	0.9864	0.9903	0.9961	4.1824	0.76	0.6821	0.7609	0.8964	1.0570
0.16	0.9823	0.9873	0.9949	3.6727	0.78	0.6690	0.7505	0.8915	1.0471
0.18	0.9776	0.9840	0.9936	3.2779	0.8	0.6560	0.7400	0.8865	1.0382
0.2	0.9725	0.9803	0.9921	2.9635	0.82	0.6430	0.7295	0.8815	1.0305
0.22	0.9668	0.9762	0.9904	2.7076	0.84	0.6300	0.7189	0.8763	1.0237
0.24	0.9607	0.9718	0.9886	2.4956	0.86	0.6170	0.7083	0.8711	1.0179
0.26	0.9541	0.9670	0.9867	2.3173	0.88	0.6041	0.6977	0.8659	1.0129
0.28	0.9470	0.9619	0.9846	2.1656	0.9	0.5913	0.6870	0.8606	1.0089
0.3	0.9395	0.9564	0.9823	2.0351	0.92	0.5785	0.6764	0.8552	1.0056
0.32	0.9315	0.9506	0.9799	1.9219	0.94	0.5658	0.6658	0.8498	1.0031
0.34	0.9231	0.9445	0.9774	1.8229	0.96	0.5532	0.6551	0.8444	1.0014
0.36	0.9143	0.9380	0.9747	1.7358	0.98	0.5407	0.6445	0.8389	1.0003
0.38	0.9052	0.9313	0.9719	1.6587	1.0	0.5283	0.6339	0.8333	1
0.4	0.8956	0.9243	0.9690	1.5901	1.02	0.5160	0.6234	0.8278	1.0003
0.42	0.8857	0.9170	0.9659	1.5289	1.04	0.5039	0.6129	0.8222	1.0013
0.44	0.8755	0.9094	0.9627	1.4740	1.06	0.4919	0.6024	0.8165	1.0029
0.46	0.8650	0.9016	0.9594	1.4246	1.08	0.4800	0.5920	0.8108	1.0051
0.48	0.8541	0.8935	0.9559	1.3801	1.1	0.4684	0.5817	0.8052	1.0079
0.5	0.8430	0.8852	0.9524	1.3398	1.12	0.4568	0.5714	0.7994	1.0113
0.52	0.8317	0.8766	0.9487	1.3034	1.14	0.4455	0.5612	0.7937	1.0153
0.54	0.8201	0.8679	0.9449	1.2703	1.16	0.4343	0.5511	0.7879	1.0198
0.56	0.8082	0.8589	0.9410	1.2403	1.18	0.4232	0.5411	0.7822	1.0248
0.58	0.7962	0.8498	0.9370	1.2130	1.2	0.4124	0.5311	0.7764	1.0304
0.6	0.7840	0.8405	0.9328	1.1882	1.22	0.4017	0.5213	0.7706	1.0366

(*Continued*)

TABLE 15.1 Isentropic Flow of a Perfect Gas ($\gamma = 1.4$)—cont'd

M	p/p_0	ρ/ρ_0	T/T_0	$A/A*$	M	p/p_0	ρ/ρ_0	T/T_0	$A/A*$
1.24	0.3912	0.5115	0.7648	1.0432	1.88	0.1539	0.2627	0.5859	1.5308
1.26	0.3809	0.5019	0.7590	1.0504	1.9	0.1492	0.2570	0.5807	1.5553
1.28	0.3708	0.4923	0.7532	1.0581	1.92	0.1447	0.2514	0.5756	1.5804
1.3	0.3609	0.4829	0.7474	1.0663	1.94	0.1403	0.2459	0.5705	1.6062
1.32	0.3512	0.4736	0.7416	1.0750	1.96	0.1360	0.2405	0.5655	1.6326
1.34	0.3417	0.4644	0.7358	1.0842	1.98	0.1318	0.2352	0.5605	1.6597
1.36	0.3323	0.4553	0.7300	1.0940	2.0	0.1278	0.2300	0.5556	1.6875
1.38	0.3232	0.4463	0.7242	1.1042	2.02	0.1239	0.2250	0.5506	1.7160
1.4	0.3142	0.4374	0.7184	1.1149	2.04	0.1201	0.2200	0.5458	1.7451
1.42	0.3055	0.4287	0.7126	1.1262	2.06	0.1164	0.2152	0.5409	1.7750
1.44	0.2969	0.4201	0.7069	1.1379	2.08	0.1128	0.2104	0.5361	1.8056
1.46	0.2886	0.4116	0.7011	1.1501	2.1	0.1094	0.2058	0.5313	1.8369
1.48	0.2804	0.4032	0.6954	1.1629	2.12	0.1060	0.2013	0.5266	1.8690
1.5	0.2724	0.3950	0.6897	1.1762	2.14	0.1027	0.1968	0.5219	1.9018
1.52	0.2646	0.3869	0.6840	1.1899	2.16	0.0996	0.1925	0.5173	1.9354
1.54	0.2570	0.3789	0.6783	1.2042	2.18	0.0965	0.1882	0.5127	1.9698
1.56	0.2496	0.3710	0.6726	1.2190	2.2	0.0935	0.1841	0.5081	2.0050
1.58	0.2423	0.3633	0.6670	1.2344	2.22	0.0906	0.1800	0.5036	2.0409
1.6	0.2353	0.3557	0.6614	1.2502	2.24	0.0878	0.1760	0.4991	2.0777
1.62	0.2284	0.3483	0.6558	1.2666	2.26	0.0851	0.1721	0.4947	2.1153
1.64	0.2217	0.3409	0.6502	1.2836	2.28	0.0825	0.1683	0.4903	2.1538
1.66	0.2151	0.3337	0.6447	1.3010	2.3	0.0800	0.1646	0.4859	2.1931
1.68	0.2088	0.3266	0.6392	1.3190	2.32	0.0775	1.1609	0.4816	2.2333
1.7	0.2026	0.3197	0.6337	1.3376	2.34	0.0751	0.1574	0.4773	2.2744
1.72	0.1966	0.3129	0.6283	1.3567	2.36	0.0728	0.1539	0.4731	2.3164
1.74	0.1907	0.3062	0.6229	1.3764	2.38	0.0706	0.1505	0.4688	2.3593
1.76	0.1850	0.2996	0.6175	1.3967	2.4	0.0684	0.1472	0.4647	2.4031
1.78	0.1794	0.2931	0.6121	1.4175	2.42	0.0663	0.1439	0.4606	2.4479
1.8	0.1740	0.2868	0.6068	1.4390	2.44	0.0643	0.1408	0.4565	2.4936
1.82	0.1688	0.2806	0.6015	1.4610	2.46	0.0623	0.1377	0.4524	2.5403
1.84	0.1637	0.2745	0.5963	1.4836	2.48	0.0604	0.1346	0.4484	2.5880
1.86	0.1587	0.2686	0.5910	1.5069	2.5	0.0585	0.1317	0.4444	2.6367

TABLE 15.1 Isentropic Flow of a Perfect Gas ($\gamma = 1.4$)—cont'd

M	p/p_0	ρ/ρ_0	T/T_0	$A/A*$	M	p/p_0	ρ/ρ_0	T/T_0	$A/A*$
2.52	0.0567	0.1288	0.4405	2.6865	3.16	0.0215	0.0643	0.3337	4.9304
2.54	0.0550	0.1260	0.4366	2.7372	3.18	0.0208	0.0630	0.3309	5.0248
2.56	0.0533	0.1232	0.4328	2.7891	3.2	0.0202	0.0617	0.3281	5.1210
2.58	0.0517	0.1205	0.4289	2.8420	3.22	0.0196	0.0604	0.3253	5.2189
2.6	0.0501	0.1179	0.4252	2.8960	3.24	0.0191	0.0591	0.3226	5.3186
2.62	0.0486	0.1153	0.4214	2.9511	3.26	0.0185	0.0579	0.3199	5.4201
2.64	0.0471	0.1128	0.4177	3.0073	3.28	0.0180	0.0567	0.3173	5.5234
2.66	0.0457	0.1103	0.4141	3.0647	3.3	0.0175	0.0555	0.3147	5.6286
2.68	0.0443	0.1079	0.4104	3.1233	3.32	0.0170	0.0544	0.3121	5.7358
2.7	0.0430	0.1056	0.4068	3.1830	3.34	0.0165	0.0533	0.3095	5.8448
2.72	0.0417	0.1033	0.4033	3.2440	3.36	0.0160	0.0522	0.3069	5.9558
2.74	0.0404	0.1010	0.3998	3.3061	3.38	0.0156	0.0511	0.3044	6.0687
2.76	0.0392	0.0989	0.3963	3.3695	3.4	0.0151	0.0501	0.3019	6.1837
2.78	0.0380	0.0967	0.3928	3.4342	3.42	0.0147	0.0491	0.2995	6.3007
2.8	0.0368	0.0946	0.3894	3.5001	3.44	0.0143	0.0481	0.2970	6.4198
2.82	0.0357	0.0926	0.3860	3.5674	3.46	0.0139	0.0471	0.2946	6.5409
2.84	0.0347	0.0906	0.3827	3.6359	3.48	0.0135	0.0462	0.2922	6.6642
2.86	0.0336	0.0886	0.3794	3.7058	3.5	0.0131	0.0452	0.2899	6.7896
2.88	0.0326	0.0867	0.3761	3.7771	3.52	0.0127	0.0443	0.2875	6.9172
2.9	0.0317	0.0849	0.3729	3.8498	3.54	0.0124	0.0434	0.2852	7.0471
2.92	0.0307	0.0831	0.3696	3.9238	3.56	0.0120	0.0426	0.2829	7.1791
2.94	0.0298	0.0813	0.3665	3.9993	3.58	0.0117	0.0417	0.2806	7.3135
2.96	0.0289	0.0796	0.3633	4.0763	3.6	0.0114	0.0409	0.2784	7.4501
2.98	0.0281	0.0779	0.3602	4.1547	3.62	0.0111	0.0401	0.2762	7.5891
3.0	0.0272	0.0762	0.3571	4.2346	3.64	0.0108	0.0393	0.2740	7.7305
3.02	0.0264	0.0746	0.3541	4.3160	3.66	0.0105	0.0385	0.2718	7.8742
3.04	0.0256	0.0730	0.3511	4.3990	3.68	0.0102	0.0378	0.2697	8.0204
3.06	0.0249	0.0715	0.3481	4.4835	3.7	0.0099	0.0370	0.2675	8.1691
3.08	0.0242	0.0700	0.3452	4.5696	3.72	0.0096	0.0363	0.2654	8.3202
3.1	0.0234	0.0685	0.3422	4.6573	3.74	0.0094	0.0356	0.2633	8.4739
3.12	0.0228	0.0671	0.3393	4.7467	3.76	0.0091	0.0349	0.2613	8.6302
3.14	0.0221	0.0657	0.3365	4.8377	3.78	0.0089	0.0342	0.2592	8.7891

(*Continued*)

TABLE 15.1 Isentropic Flow of a Perfect Gas ($\gamma = 1.4$)—cont'd

M	p/p_0	ρ/ρ_0	T/T_0	$A/A*$	M	p/p_0	ρ/ρ_0	T/T_0	$A/A*$
3.8	0.0086	0.0335	0.2572	8.9506	4.42	0.0038	0.0187	0.2038	15.4724
3.82	0.0084	0.0329	0.2552	9.1148	4.44	0.0037	0.0184	0.2023	15.7388
3.84	0.0082	0.0323	0.2532	0.2817	4.46	0.0036	0.0181	0.2009	16.0092
3.86	0.0080	0.0316	0.2513	9.4513	4.48	0.0035	0.0178	0.1994	16.2837
3.88	0.0077	0.0310	0.2493	9.6237	4.5	0.0035	0.0174	0.1980	16.5622
3.9	0.0075	0.0304	0.2474	9.7990	4.52	0.0034	0.0171	0.1966	16.8449
3.92	0.0073	0.0299	0.2455	9.9771	4.54	0.0033	0.0168	0.1952	17.1317
3.94	0.0071	0.0293	0.2436	10.1581	4.56	0.0032	0.0165	0.1938	17.4228
3.96	0.0069	0.0287	0.2418	10.3420	4.58	0.0031	0.0163	0.1925	17.7181
3.98	0.0068	0.0282	0.2399	10.5289	4.6	0.0031	0.0160	0.1911	18.0178
4.0	0.0066	0.0277	0.2381	10.7188	4.62	0.0030	0.0157	0.1898	18.3218
4.02	0.0064	0.0271	0.2363	10.9117	4.64	0.0029	0.0154	0.1885	18.6303
4.04	0.0062	0.0266	0.2345	11.1077	4.66	0.0028	0.0152	0.1872	18.9433
4.06	0.0061	0.0261	0.2327	11.3068	4.68	0.0028	0.0149	0.1859	19.2608
4.08	0.0059	0.0256	0.2310	11.5091	4.7	0.0027	0.0146	0.1846	19.5828
4.1	0.0058	0.0252	0.2293	11.7147	4.72	0.0026	0.0144	0.1833	19.9095
4.12	0.0056	0.0247	0.2275	11.9234	4.74	0.0026	0.0141	0.1820	20.2409
4.14	0.0055	0.0242	0.2258	12.1354	4.76	0.0025	0.0139	0.1808	20.5770
4.16	0.0053	0.0238	0.2242	12.3508	4.78	0.0025	0.0137	0.1795	20.9179
4.18	0.0052	0.0234	0.2225	12.5695	4.8	0.0024	0.0134	0.1783	21.2637
4.2	0.0051	0.0229	0.2208	12.7916	4.82	0.0023	0.0132	0.1771	21.6144
4.22	0.0049	0.0225	0.2192	13.0172	4.84	0.0023	0.0130	0.1759	21.9700
4.24	0.0048	0.0221	0.2176	13.2463	4.86	0.0022	0.0128	0.1747	22.3306
4.26	0.0047	0.0217	0.2160	13.4789	4.88	0.0022	0.0125	0.1735	22.6963
4.28	0.0046	0.0213	0.2144	13.7151	4.9	0.0021	0.0123	0.1724	23.0671
4.3	0.0044	0.0209	0.2129	13.9549	4.92	0.0021	0.0121	0.1712	23.4431
4.32	0.0043	0.0205	0.2113	14.1984	4.94	0.0020	0.0119	0.1700	23.8243
4.34	0.0042	0.0202	0.2098	14.4456	4.96	0.0020	0.0117	0.1689	24.2109
4.36	0.0041	0.0198	0.2083	14.6965	4.98	0.0019	0.0115	0.1678	24.6027
4.38	0.0040	0.0194	0.2067	14.9513	5.0	0.0019	0.0113	0.1667	25.0000
4.4	0.0039	0.0191	0.2053	15.2099					

a high-speed stream is decelerated and compressed. For example, air may enter the jet engine of an aircraft after passing through a diffuser, which raises the pressure and temperature of the air. In incompressible flow, a nozzle profile converges in the direction of flow to increase the flow velocity, while a diffuser profile diverges. We shall see that such convergence and divergence must be reversed for supersonic flows in nozzles and diffusers.

Conservation of mass for compressible flow in a duct with smoothly varying area is specified by (15.19). For constant density flow $d\rho/dx = 0$ and (15.19) implies $dA/dx + du/dx = 0$, so a decreasing area leads to an increase of velocity. When the flow is compressible, frictionless, and adiabatic then (15.26) implies

$$udu = -dp/\rho = c^2 d\rho/\rho, \tag{15.32}$$

because the flow is isentropic under these circumstances. Thus, the Euler equation requires that an increasing speed ($du > 0$) in the direction of flow must be accompanied by a fall of pressure ($dp < 0$). In terms of the Mach number, (15.32) becomes

$$d\rho/\rho = -M^2 du/u. \tag{15.33}$$

This shows that for $M \ll 1$, the percentage change of density is much smaller than the percentage change of velocity. The density changes in the continuity equation (15.19) can therefore be neglected in low Mach number flows, a fact also mentioned in Section 15.1. Substituting (15.33) into (15.19), we obtain a velocity-area differential relationship that is valid in compressible flow:

$$\frac{du}{u} = -\frac{1}{1 - M^2}\frac{dA}{A}. \tag{15.34}$$

This relation leads to the following important conclusions about compressible flows:

(i) At subsonic speeds ($M < 1$) a decrease of area increases the speed of flow. A subsonic nozzle therefore must have a convergent profile, and a subsonic diffuser must have a divergent profile (upper row of Figure 15.4). The behavior is qualitatively the same as in incompressible ($M = 0$) flows.

(ii) At supersonic speeds ($M > 1$) the denominator in (15.34) is negative, and we arrive at the conclusion that an *increase* in area leads to an increase of speed. The reason for such a behavior can be understood from (15.33), which shows that for $M > 1$ the density decreases faster than the velocity increases, thus the area must increase in an accelerating flow in order for ρuA to remain constant.

Therefore, the supersonic portion of a nozzle must have a divergent profile, and the supersonic part of a diffuser must have a convergent profile (bottom row of Figure 15.4).

Suppose a nozzle is used to generate a supersonic stream, starting from a low-speed, high-pressure air stream at its inlet (Figure 15.5). Then the Mach number must increase continuously from $M = 0$ near the inlet to $M > 1$ at the exit. The foregoing discussion shows that the nozzle must converge in the subsonic portion and diverge in the supersonic portion. Such a nozzle is called a *convergent–divergent nozzle*. From Figure 15.5 it is clear that the Mach number must be unity at the *throat*, where the area is neither increasing nor decreasing ($dA \to 0$). This is consistent with (15.34), which shows that du can be nonzero at the throat

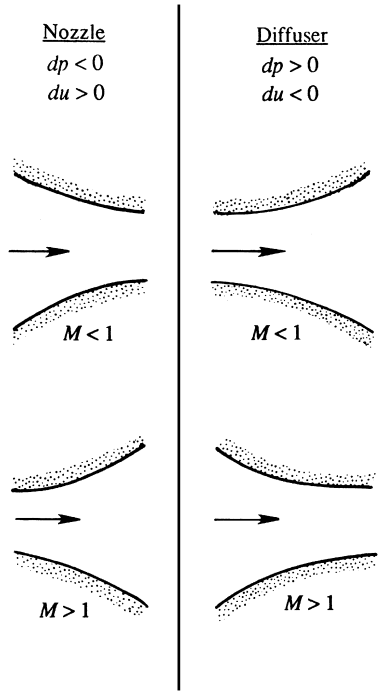

FIGURE 15.4 Shapes of nozzles and diffusers in subsonic and supersonic regimes. Nozzles are devices that accelerate the flow and are shown in the left column. Diffusers are devices that decelerate the flow and are shown in the right column. The area change with increasing downstream distance, dA/dx, switches sign for nozzles and diffusers and when the flow switches from subsonic to supersonic.

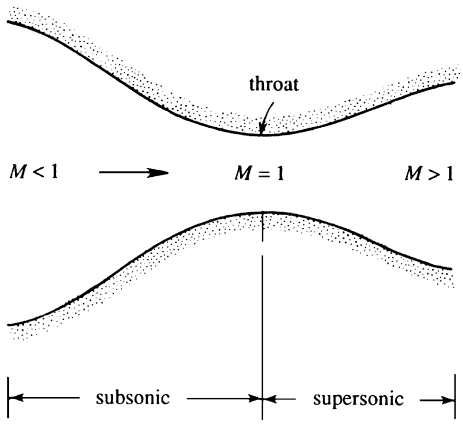

FIGURE 15.5 A convergent–divergent nozzle. When the pressure difference between the nozzle inlet and outlet is large enough, a compressible flow may be continuously accelerated from low speed to a supersonic Mach number through such a nozzle. When this happens the Mach number is unity at the minimum area, known as the nozzle's *throat*.

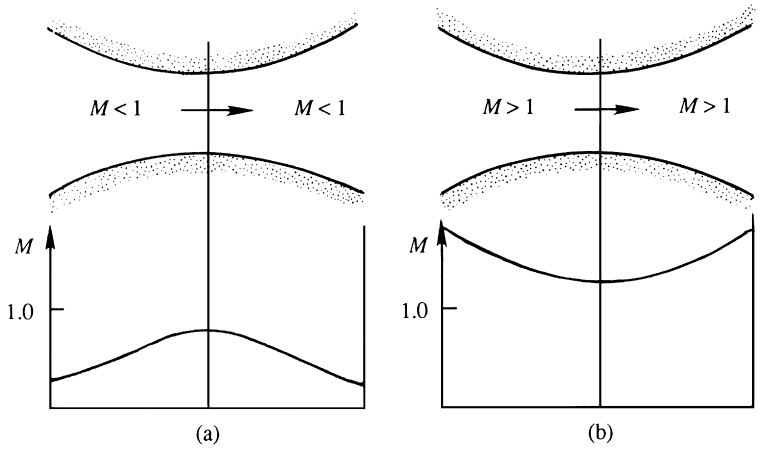

FIGURE 15.6 Convergent–divergent passages in which the condition at the throat is not sonic. This occurs when the flow is entirely subsonic as in (a), and when it is entirely supersonic as in (b).

only if $M = 1$. It follows that the *sonic velocity can be achieved only at the throat of a nozzle or a diffuser and nowhere else*.

It does not, however, follow that M must necessarily be unity at the throat. According to (15.34), we may have a case where $M \neq 1$ at the throat if $du = 0$ there. As an example, the flow in a convergent–divergent tube may be subsonic everywhere, with M increasing in the convergent portion and decreasing in the divergent portion, with $M \neq 1$ at the throat (Figure 15.6a). In this case the nozzle may also be known as a *venturi tube*. For entirely subsonic flow, the first half of the tube here is acting as a nozzle, whereas the second half is acting as a diffuser. Alternatively, we may have a convergent–divergent tube in which the flow is supersonic everywhere, with M decreasing in the convergent portion and increasing in the divergent portion, and again $M \neq 1$ at the throat (Figure 15.6b).

EXAMPLE 15.1

The nozzle of a rocket motor is designed to generate a thrust of 30,000 N when operating at an altitude of 20 km. The pressure and temperature inside the combustion chamber are 1000 kPa and 2500 K. The gas constant of the fluid in the jet is $R = 280\ \mathrm{m^2/(s^2K)}$, and $\gamma = 1.4$. Assuming that the flow in the nozzle is isentropic, calculate the throat and exit areas. Use the isentropic table (Table 15.1).

Solution

At an altitude of 20 km, the pressure of the standard atmosphere (Section A.4 in Appendix A) is 5467 Pa. If subscripts 0 and e refer to the stagnation and exit conditions, then a summary of the information given is as follows:

$$p_e = 5467\ \mathrm{Pa}, p_0 = 1000\ \mathrm{kPa},\ T_0 = 2500\ \mathrm{K}, \quad \text{and} \quad \text{Thrust} = \rho_e u_e^2 A_e = 30\ \mathrm{kN}.$$

Here, we have used the facts that the thrust equals mass flow rate times the exit velocity, and the pressure inside the combustion chamber is nearly equal to the stagnation pressure. The pressure ratio at the exit is

$$\frac{p_e}{p_0} = \frac{5467}{(1000)(1000)} = 5.467 \times 10^{-3}.$$

For this ratio of p_e/p_0, the isentropic table (Table 15.1) gives:

$$m_e = 4.15,\ A_e/A^* = 12.2, \quad \text{and} \quad T_e/T_0 = 0.225.$$

The exit temperature and density are therefore:

$$\begin{aligned} T_e &= (0.225)(2500) = 562\ \text{K}, \\ \rho_e &= p_e/RT_e = 5467/(280)(562) = 0.0347\ \text{kg/m}^3. \end{aligned}$$

The exit velocity is

$$u_e = M_e\sqrt{\gamma RT_e} = 4.15\sqrt{(1.4)(280)(562)} = 1948\ \text{m/s}.$$

The exit area is found from the expression for thrust:

$$A_e = \frac{\text{Thrust}}{\rho_e u_e^2} = \frac{30,000}{(0.0347)(1948)^2} = 0.228\ \text{m}^2.$$

Because $A_e/A^* = 12.2$, the throat area is

$$A^* = \frac{0.228}{12.2} = 0.0187\ \text{m}^2.$$

15.6. NORMAL SHOCK WAVES

A shock wave is similar to a step-change compression sound wave except that it has finite strength. The thickness of such waves is typically of the order of micrometers, so that fluid properties vary almost discontinuously across a shock wave. The high gradients of velocity and temperature result in entropy production within the wave so isentropic relations cannot be used across a shock. This section presents the relationships between properties of the flow upstream and downstream of a *normal shock*, where the shock is perpendicular to the direction of flow. The shock wave is treated as a discontinuity and the actual process by which entropy is generated is not addressed. However, the entropy rise across the shock predicted by this analysis is correct. The internal structure of a shock as predicted by the Navier-Stokes equations under certain simplifying assumptions is given at the end of this section.

Stationary Normal Shock Wave in a Moving Medium

To get started, consider a thin control volume shown in Figure 15.7 that encloses a stationary shock wave. The control surface locations 1 and 2, shown as dashed lines in

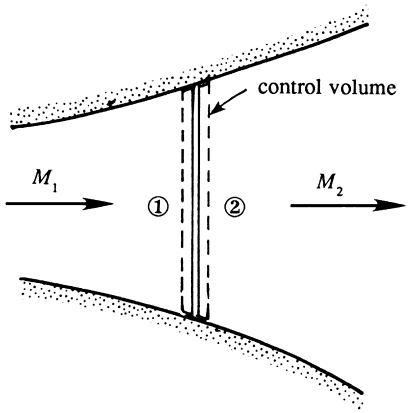

FIGURE 15.7 A normal shock wave trapped in a steady nozzle flow. Here a control volume is shown that has control surfaces immediately upstream (1) and downstream (2) of the shock wave. Shock waves are very thin in most gases, so the area change and wall friction of the duct need not be considered as the flow traverses the shock wave.

the figure, can be taken close to each other because of the discontinuous nature of the wave. In this case, the area change and the wall-surface friction between the upstream and the downstream control volume surfaces can be neglected. Furthermore, external heat addition is not of interest here so the basic equations are (15.18) and (15.24) with $F = 0$, both simplified for constant area, and (15.22) with $Q = 0$:

$$\rho_1 u_1 = \rho_2 u_2,\ p_1 - p_2 = -\rho_1 u_1^2 + \rho_2 u_2^2, \quad \text{and} \quad h_1 + \frac{1}{2}u_1^2 = h_2 + \frac{1}{2}u_2^2. \quad (15.35, 15.36, 15.37)$$

The Bernoulli equation cannot be used here because the process inside the shock wave is dissipative. The equations (15.35) through (15.37) contain four unknowns (h_2, u_2, p_2, ρ_2). The additional relationship comes from the thermodynamics of a perfect gas (15.1):

$$h = C_p T = \frac{\gamma R}{\gamma - 1}\frac{p}{\rho R} = \frac{\gamma p}{(\gamma - 1)\rho},$$

so that (15.37) becomes

$$\frac{\gamma}{\gamma - 1}\frac{p_1}{\rho_1} + \frac{1}{2}u_1^2 = \frac{\gamma}{\gamma - 1}\frac{p_2}{\rho_2} + \frac{1}{2}u_2^2. \quad (15.38)$$

There are now three unknowns (u_2, p_2, ρ_2) and three equations: (15.35), (15.36), and (15.38), so the remainder of the effort to link the conditions upstream and downstream of a shock is primarily algebraic. Elimination of ρ_2 and u_2 from these gives, after some algebra:

$$\frac{p_2}{p_1} = 1 + \frac{2\gamma}{\gamma + 1}\left[\frac{\rho_1 u_1^2}{\gamma p_1} - 1\right].$$

This can be expressed in terms of the upstream Mach number M_1 by noting that $\rho u^2/\gamma p = u^2/\gamma RT = M^2$. The pressure ratio then becomes

$$\frac{p_2}{p_1} = 1 + \frac{2\gamma}{\gamma+1}(M_1^2 - 1). \tag{15.39}$$

Let us now derive a relation between M_1 and M_2. Because $\rho u^2 = \rho c^2 M^2 = \rho(\gamma p/\rho)M^2 = \gamma p M^2$, the momentum equation (15.36) can be written

$$p_1 + \gamma p_1 M_1^2 = p_2 + \gamma p_2 M_2^2.$$

Using (15.39), this gives

$$M_2^2 = \frac{(\gamma-1)M_1^2 + 2}{2\gamma M_1^2 + 1 - \gamma}, \tag{15.40}$$

which is plotted in Figure 15.8. Because $M_2 = M_1$ (state 2 = state 1) is a solution of (15.35), (15.36), and (15.38), that is shown as well, indicating two possible solutions for M_2 for all $M_1 > [(\gamma-1)/2\gamma]^{1/2}$. As is shown below, M_1 must be greater than unity to avoid violation of the second law of thermodynamics, so the two possibilities for the downstream state are: 1) no change from upstream, and 2) a sudden transition from supersonic to subsonic flow with consequent increases in pressure, density, and temperature. The density, velocity, and temperature ratios can be similarly obtained from the equations provided so far. They are:

$$\frac{\rho_2}{\rho_1} = \frac{u_1}{u_2} = \frac{(\gamma+1)M_1^2}{(\gamma-1)M_1^2 + 2}, \tag{15.41}$$

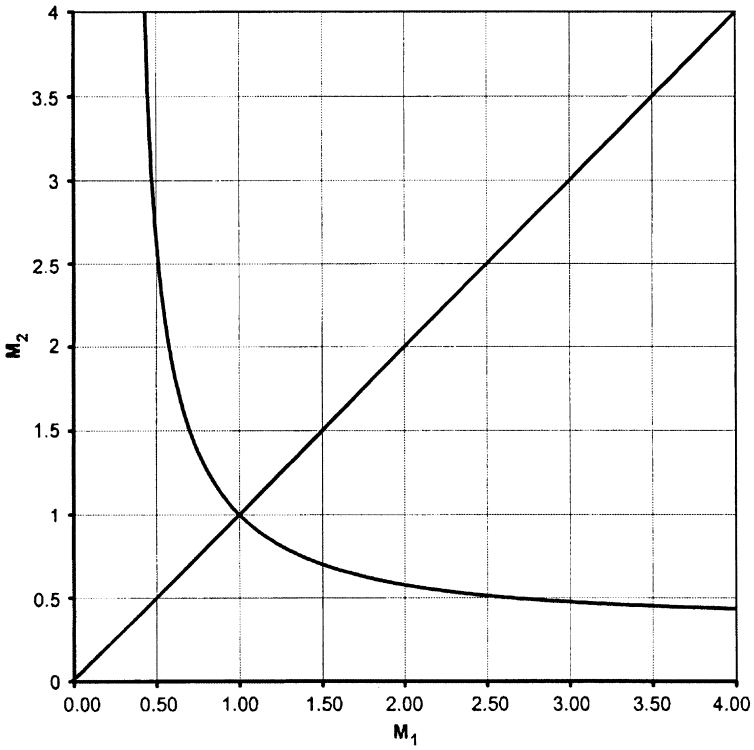

FIGURE 15.8 Normal shock-wave solution for M_2 as function of M_1 for $\gamma = 1.4$. The trivial (no change) solution is also shown as the straight line with unity slope. Asymptotes are $[(\gamma-1)/2\gamma]^{1/2} = 0.378$ for M_1 or $M_2 \to \infty$. The second law of thermodynamics limits valid shock-wave solutions to those having $M_1 > 1$.

$$\frac{T_2}{T_1} = 1 + \frac{2(\gamma-1)}{(\gamma+1)^2}\frac{\gamma M_1^2 + 1}{M_1^2}(M_1^2 - 1). \tag{15.42}$$

The normal shock relations (15.39) through (15.43) were worked out independently by the British engineer W. J. M. Rankine (1820–1872) and the French ballistician Pierre Henry Hugoniot (1851–1887). These equations are sometimes known as the *Rankine-Hugoniot relations*.

An important quantity is the change of entropy across the shock. Using (15.1), the entropy change is

$$\frac{S_2 - S_1}{C_v} = \ln\left[\frac{p_2}{p_1}\left(\frac{\rho_1}{\rho_2}\right)^{\gamma}\right] = \ln\left\{\left[1 + \frac{2\gamma}{\gamma+1}(M_1^2 - 1)\right]\left[\frac{(\gamma-1)M_1^2 + 2}{(\gamma+1)M_1^2}\right]^{\gamma}\right\}, \tag{15.43}$$

which is plotted in Figure 15.9. This figure shows that the entropy change across an expansion shock in a perfect gas would decrease, which is impermissible. However, expansion shocks may be possible when the gas follows a different equation of state (Fergason et al., 2001). When the upstream Mach number is close to unity, Figure 15.9 shows that the entropy change may be very small. The dependence of $S_2 - S_1$ on M_1 in the neighborhood of $M_1 = 1$ can be ascertained by treating $M_1^2 - 1$ as a small quantity and expanding (15.43) in terms of it (see Exercise 15.5) to find:

$$\frac{S_2 - S_1}{C_v} \cong \frac{2\gamma(\gamma-1)}{3(\gamma+1)^2}(M_1^2 - 1)^3. \tag{15.44a}$$

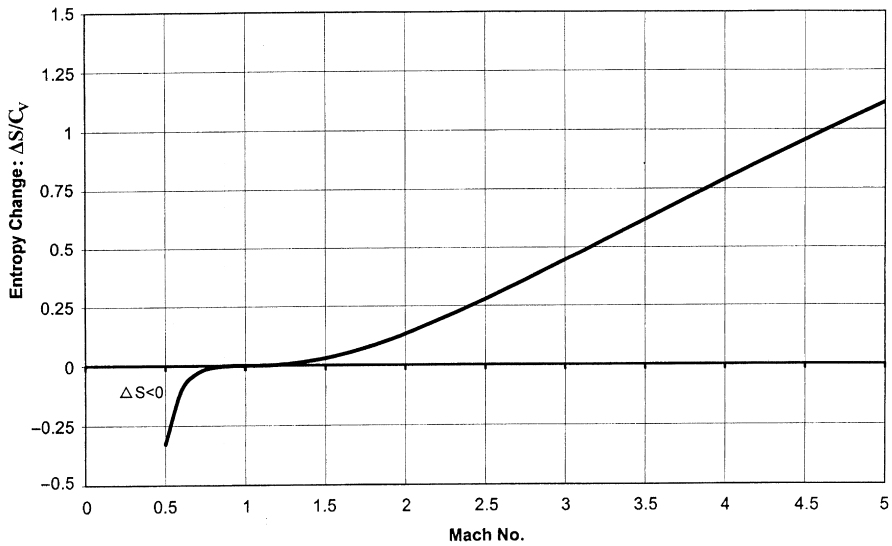

FIGURE 15.9 Entropy change $(S_2 - S_1)/C_v$ as a function of M_1 for $\gamma = 1.4$. Note higher-order contact at $M = 1$ to the horizontal line corresponding to zero entropy change as $M_1 \to 1$ from above. Negative entropy changes are predicted for $M_1 < 1$, so shock waves do not occur unless the upstream speed is supersonic, $M_1 > 1$.

This equation explicitly shows that $S_2 - S_1$ will only be positive for a perfect gas when $M_1 > 1$. Thus, stationary shock waves do not occur when $M_1 < 1$ because of the second law of thermodynamics. However, when $M_1 > 1$, then (15.40) requires that $M_2 < 1$. Thus, the *Mach number changes from supersonic to subsonic values across a normal shock*, and this is the only possibility. A shock wave is therefore analogous to a hydraulic jump (see Section 7.6) in a gravity current, in which the Froude number jumps from supercritical to subcritical values; see Figure 7.20. Equations (15.39), (15.41), and (15.42) then show that the jumps in p, ρ, and T are also from lower to higher values, so that a shock wave leads to compression and heating of a fluid at the expense of streamwise velocity.

Interestingly, terms involving the first two powers of $(M_1^2 - 1)$ do not appear in (15.44a). Using the pressure ratio from (15.39), (15.44a) can be rewritten:

$$\frac{S_2 - S_1}{C_v} \cong \frac{\gamma^2 - 1}{12\gamma^2}\left(\frac{p_2 - p_1}{p_1}\right)^3. \tag{15.44b}$$

This shows that as the wave amplitude $\Delta p = p_2 - p_1$ decreases the entropy jump goes to zero like $(\Delta p)^3$. Thus weak shock waves are nearly isentropic and this is the primary reason that loud acoustic disturbances are successfully treated as isentropic. Because of the adiabatic nature of the process, the stagnation properties T_0 and h_0 are constant across the shock. In contrast, the stagnation properties p_0 and ρ_0 decrease across the shock due to the dissipative processes inside the wave front.

Moving Normal Shock Wave in a Stationary Medium

Frequently, one needs to calculate the properties of flow due to the propagation of a shock wave through a still medium, for example, that caused by an explosion. The Galilean transformation necessary to analyze this problem is indicated in Figure 15.10. The left panel shows a stationary shock, with incoming and outgoing velocities u_1 and

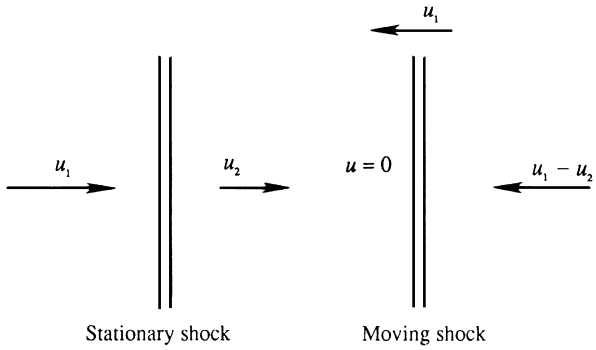

FIGURE 15.10 Stationary and moving shocks. The stationary shock shown in the left panel corresponds to a situation like that depicted in Figure 15.7 where the incoming flow moves toward the shock. The moving shock situation shown on the right corresponds to a blast wave that propagates away from an explosion into still air.

u_2, respectively. To this flow we add a velocity u_1 directed to the left, so that the fluid entering the shock is stationary, and the fluid downstream of the shock is moving to the *left* at a speed $u_1 - u_2$, as shown in the right panel of the figure. This is consistent with acoustic results in Section 15.2 where it was found that the fluid within a compression wave moves in the direction of wave propagation. The shock speed is therefore u_1, with a supersonic Mach number $M_1 = u_1/c_1 > 1$. It follows that a *finite pressure disturbance propagates through a still fluid at supersonic speed*, in contrast to infinitesimal waves that propagate at the sonic speed. The expressions for all the thermodynamic properties of the flow, such as (15.39) through (15.44), are still applicable.

Normal Shock Structure

We conclude this section on normal shock waves with a look into the structure of a shock wave. The viscous and heat conductive processes within the shock wave result in an entropy increase across the wave. However, the magnitudes of the viscosity μ and thermal conductivity k only determine the thickness of the shock wave and not the magnitude of the entropy increase. The entropy increase is determined solely by the upstream Mach number as shown by (15.43). We shall also see later that the *wave drag* experienced by a body due to the appearance of a shock wave is independent of viscosity or thermal conductivity. (The situation here is analogous to the viscous dissipation in fully turbulent flows, Section 12.7, in which the average kinetic-energy dissipation rate $\overline{\varepsilon}$ is determined by the velocity and length scales of a large-scale turbulence field (12.49) and not by the magnitude of the viscosity; a change in viscosity merely changes the length scale at which the dissipation takes place, namely, the Kolmogorov microscale.)

A shock wave can be considered a very thin boundary layer involving a large stream-wise velocity gradient du/dx, in contrast to the cross-stream (or wall-normal) velocity gradient involved in a viscous boundary layer near a solid surface. Analysis shows that the thickness δ of a shock wave is given by

$$(u_1 - u_2)\delta/\nu \sim 1,$$

where the left side is a Reynolds number based on the velocity change across the shock, its thickness, and the average kinematic viscosity. Taking a typical value for air of $\nu \sim 10^{-5}$ m^2/s, and a velocity jump of $\Delta u \sim 100$ m/s, we obtain a shock thickness of 10^{-7} m. This is not much larger than the mean free path (average distance traveled by a molecule between collisions), which suggests that the continuum hypothesis and the assumption of local thermodynamic equilibrium are both of questionable validity in analyzing shock structure.

With these limitations noted, some insight into the structure of shock waves may be gained by considering the one-dimensional steady Navier-Stokes equations, including heat conduction and Newtonian viscous stresses, in a shock-fixed coordinate system. The solution we obtain provides a smooth transition between upstream and downstream states, looks reasonable, and agrees with experiments and kinetic theory models for upstream Mach numbers less than about 2. The equations for conservation of mass, momentum, and energy,

respectively, are the steady one-dimensional versions of (4.7), (4.38) without a body force, and (4.60) written in terms of enthalpy h:

$$\frac{d(\rho u)}{dx} = 0,\ \rho u\frac{du}{dx} + \frac{dp}{dx} = \frac{d}{dx}\left(\left(\frac{4}{3}\mu + \mu_v\right)\frac{du}{dx}\right), \quad \text{and}$$
$$\rho u\frac{dh}{dx} - u\frac{dp}{dx} = \left(\frac{4}{3}\mu + \mu_v\right)\left(\frac{du}{dx}\right)^2 + \frac{d}{dx}\left(k\frac{dT}{dx}\right).$$

By adding the product of u and the momentum equation to the energy equation, these can be integrated once to find:

$$\rho u = m,\ mu + p = \mu''\frac{du}{dx} + mV, \quad \text{and} \quad m\left(h + \frac{1}{2}u^2\right) = \mu'' u\frac{du}{dx} + k\frac{dT}{dx} + mI,$$

where m, V, and I are the constants of integration and $\mu'' = (4/3)\mu + \mu_v$. When these are evaluated upstream (state 1) and downstream (state 2) of the shock where gradients vanish, they yield the Rankine-Hugoniot relations derived earlier. We also need the equations of state for a perfect gas with constant specific heats to solve for the structure: $h = C_p T$, and $p = \rho RT$. Multiplying the energy equation by C_p/k we obtain the form:

$$m\frac{C_p}{k}\left(C_p T + \frac{1}{2}u^2\right) = \frac{\mu'' C_p}{2k}\frac{du^2}{dx} + C_p\frac{dT}{dx} + m\frac{C_p}{k}I.$$

This equation has an exact integral in the special case $\mathrm{Pr}'' \equiv \mu'' C_p/k = 1$ that was found by Becker in 1922. For most simple gases, Pr'' is likely to be near unity so it is reasonable to proceed assuming $\mathrm{Pr}'' = 1$. The Becker integral is $C_p T + u^2/2 = I$. Eliminating all variables but u from the momentum equation, using the equations of state, mass conservation, and the energy integral, we reach:

$$mu + (m/u)\left(R/C_p\right)\left(I - u^2/2\right) - \mu''\, du/dx = mV.$$

With $C_p/R = \gamma/(\gamma - 1)$, multiplying by u/m leads to

$$-\left[2\gamma/(\gamma+1)\right](\mu''/m)u\,du/dx = -u^2 + \left[2\gamma/(\gamma+1)\right]uV - 2I\left(\gamma - 1\right)/\left(\gamma + 1\right)$$
$$\equiv \left(U_1 - U\right)\left(U - U_2\right).$$

Divide by V^2 and let $u/V = U$. The equation for the structure becomes

$$-U(U_1 - U)^{-1}(U - U_2)^{-1}dU = [(\gamma+1)/2\gamma](m/\mu'')dx,$$

where the roots of the quadratic are

$$U_{1,2} = [\gamma/(\gamma+1)]\left\{1 \pm \left[1 - 2\left(\gamma^2 - 1\right)I/\left(\gamma^2 V^2\right)\right]^{1/2}\right\},$$

the dimensionless speeds far up- and downstream of the shock. The left-hand side of the equation for the structure is rewritten in terms of partial fractions and then integrated to obtain

$$[U_1 \ln(U_1 - U) - U_2 \ln(U - U_2)]/(U_1 - U_2) = [(\gamma+1)/(2\gamma)]m\int dx/\mu'' \equiv [(\gamma+1)/(2\gamma)]\eta.$$

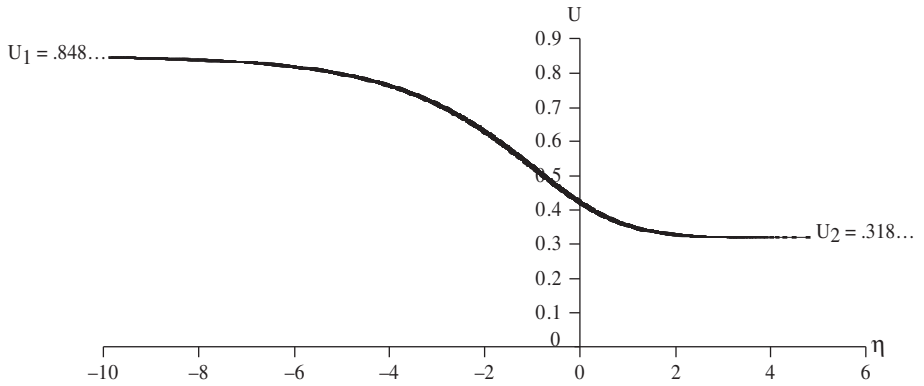

FIGURE 15.11 Shock structure velocity profile for the case $U_1 = 0.848485$, $U_2 = 0.31818$, corresponding to $M_1 = 2.187$. The units of the horizontal coordinate may be approximately interpreted as mean-free paths. Thus, a shock wave is typically a small countable number of mean-free-paths thick.

The resulting shock structure is shown in Figure 15.11 in terms of the stretched coordinate $\eta = \int (m/\mu'')dx$ where μ'' is often a strong function of temperature and thus of x. A similar structure is obtained for all except quite small values of Pr″. In the limit Pr″ $\rightarrow$ 0, Hayes (1958) points out that there must be a "shock within a shock" because heat conduction alone cannot provide the entire structure. In fact, Becker (1922, footnote, p. 341) credits Prandtl for originating this idea. Cohen and Moraff (1971) provided the structure of both the outer (heat conducting) and inner (isothermal viscous) shocks. Here, the variable η is a dimensionless length scale measured very roughly in units of mean free paths. We see that a measure of shock thickness is of the order of 5 mean free paths from this analysis.

15.7. OPERATION OF NOZZLES AT DIFFERENT BACK PRESSURES

Nozzles are used to accelerate a fluid stream and are employed in such systems as wind tunnels, rocket motors, ejector pumps, and steam turbines. A pressure drop is maintained across the nozzle to accelerate fluid through it. This section presents the behavior of the flow through a nozzle as the back pressure p_B on the nozzle is varied when the nozzle-supply pressure is maintained at a constant value p_0 (the stagnation pressure). Here the p_B is the pressure in the nominally quiescent environment into which the nozzle flow is directed. In the following discussion, the pressure p_{exit} at the exit plane of the nozzle equals the back pressure p_B if the flow at the exit plane is subsonic, but *not* if it is supersonic. This must be true because subsonic flow allows the downstream pressure p_B to be communicated up into the nozzle exit, and sharp pressure changes are only allowed in a supersonic flow.

Convergent Nozzle

Consider first the case of a convergent nozzle shown in Figure 15.12, which examines a sequence of states *a* through *c* during which the back pressure is gradually lowered.

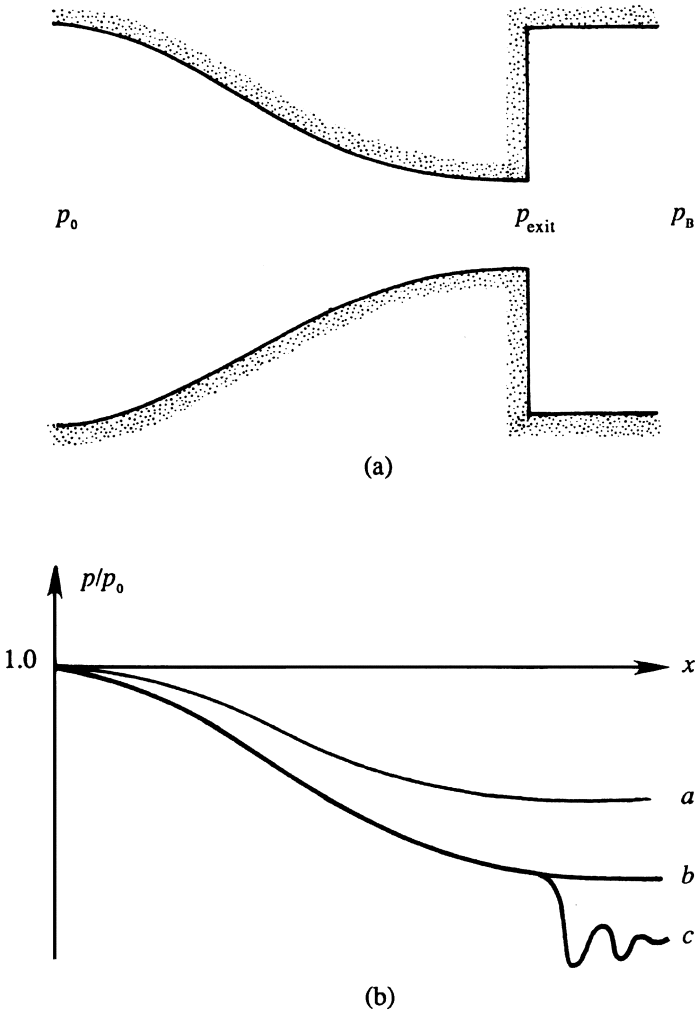

FIGURE 15.12 Pressure distribution along a convergent nozzle for different values of back pressure p_B: (a) diagram of the nozzle, and (b) pressure distributions as p_B is lowered. Here the highest possible flow speed at the nozzle exit is sonic. When p_B is lowered beyond the point of sonic flow at the nozzle exit, the flow continues to accelerate outside the nozzle via expansion waves that lead to nonuniform pressures (curve *c*).

For curve *a*, the flow throughout the nozzle is subsonic. As p_B is lowered, the Mach number increases everywhere and the mass flux through the nozzle also increases. This continues until sonic conditions are reached at the exit, as represented by curve *b*. Further lowering of the back pressure has no effect on the flow inside the nozzle. This is because the fluid at the exit is now moving downstream at the velocity at which no pressure changes can propagate upstream. Changes in p_B therefore cannot propagate upstream after sonic conditions are reached at the nozzle exit. We say that the nozzle at this stage is *choked* because the mass flux cannot be increased by further lowering of back pressure. If p_B is lowered further (curve *c* in Figure 15.12), supersonic flow is generated downstream of the nozzle, and the jet pressure adjusts to p_B by means of a series of oblique compression and expansion waves, as schematically indicated by the oscillating pressure distribution

for curve *c*. Oblique compression and expansion waves are explained in Sections 15.9 and 15.10. It is only necessary to note here that they are oriented at an angle to the direction of flow, and that the pressure increases through an oblique compression wave and decreases through an oblique expansion wave.

Convergent–Divergent Nozzle

Now consider the case of a convergent–divergent passage, also known as a Laval nozzle (Figure 15.13). Completely subsonic flow applies to curve *a*. As p_B is lowered to p_b, the sonic

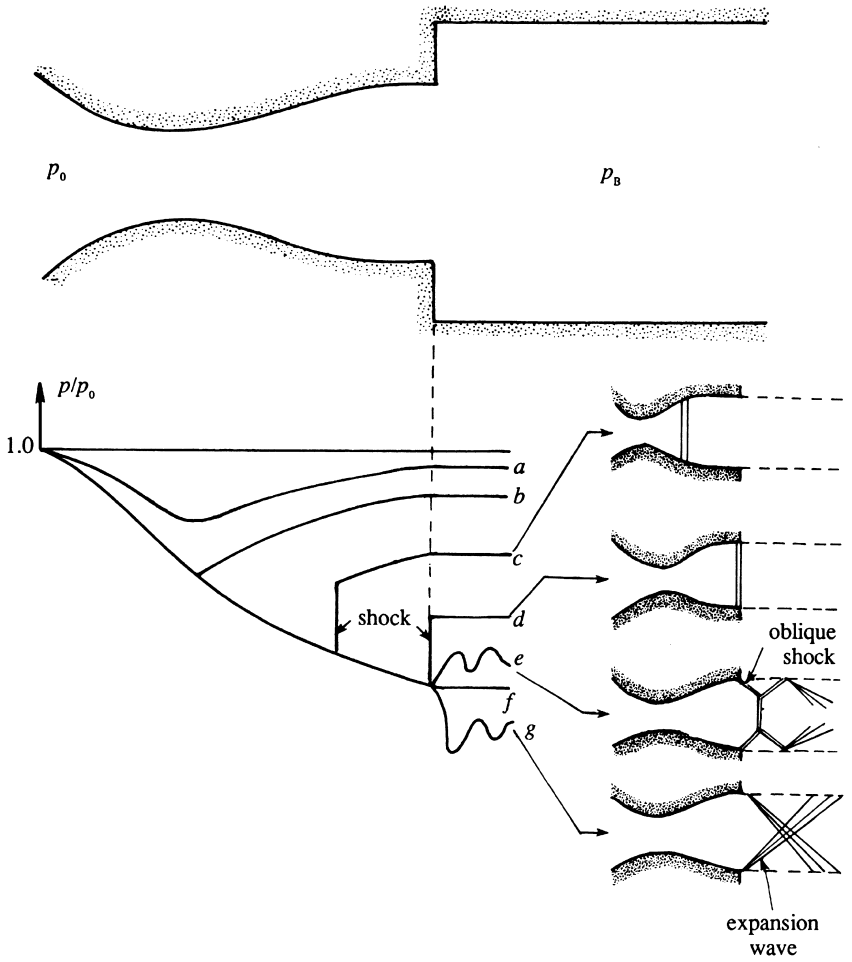

FIGURE 15.13 Pressure distribution along a convergent–divergent (aka Laval) nozzle for different values of the back pressure p_B. Flow patterns for cases *c*, *d*, *e*, and *g* are indicated schematically on the right. The condition *f* is the *pressure matched* case and usually corresponds to the nozzle's design condition. For this case, the flow looks like that of *c* or *d* without the shock wave. *H. W. Liepmann and A. Roshko,* Elements of Gas Dynamics, *Wiley, New York, 1957; reprinted with the permission of Dr. Anatol Roshko.*

condition is reached at the throat. On further reduction of the back pressure, the flow upstream of the throat does not respond, and the nozzle flow is choked in the sense that it has reached the maximum mass flow rate for the given values of p_0 and throat area. There is a range of back pressures, shown by curves c and d, in which the flow initially becomes supersonic in the divergent portion, but then adjusts to the back pressure by means of a normal shock standing inside the nozzle. The flow downstream of the shock is, of course, subsonic. In this range the position of the shock moves downstream as p_B is decreased, and for curve d the normal shock stands right at the exit plane. The flow in the entire divergent portion up to the exit plane is now supersonic and remains so on further reduction of p_B. When the back pressure is further reduced to p_e, there is no normal shock anywhere within the nozzle, and the jet pressure adjusts to p_B by means of oblique compression waves downstream of the nozzle's exit plane. These oblique waves vanish when $p_B = p_f$. On further reduction of the back pressure, the adjustment to p_B takes place outside the exit plane by means of oblique expansion waves.

EXAMPLE 15.2

A convergent–divergent nozzle is operating under off-design conditions, resulting in the presence of a shock wave in the diverging portion. A reservoir containing air at 400 kPa and 800 K supplies the nozzle, whose throat area is 0.2 m^2. The Mach number upstream of the shock is $M_1 = 2.44$. The area at the nozzle exit is 0.7 m^2. Find the area at the location of the shock and the exit temperature.

Solution

Figure 15.14 shows the profile of the nozzle, where sections 1 and 2 represent conditions across the shock. As a shock wave can exist only in a supersonic stream, we know that sonic conditions are reached at the throat, and the throat area equals the critical area A^*. The values given are therefore:

$$p_0 = 400 \text{ kPa},\ T_0 = 800 \text{ K},\ A_{throat} = A_1^* = 0.2 \text{ m}^2,\ M_1 = 2.44, \quad \text{and} \quad A_3 = 0.7 \text{ m}^2.$$

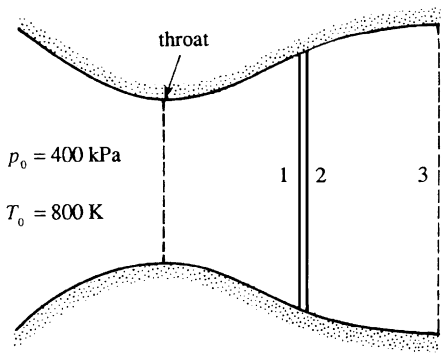

FIGURE 15.14 Drawing for Example 15.2. This is case c from Figure 15.13 where a normal shock occurs in the nozzle.

Note that A^* is constant upstream of the shock because the flow is isentropic there; this is why $A_{\text{throat}} = A_1^*$.

The technique of solving this problem is to proceed downstream from the given stagnation conditions. For $M_1 = 2.44$, the isentropic table Table 15.1 gives:

$$A_1/A_1^* = 2.5, \text{ so that } A_1 = A_2 = (2.5)(0.2) = 0.5 \text{ m}^2.$$

This is the nozzle's cross-section area at the location of the shock. For $M_1 = 2.44$, the normal shock Table 15.2 gives:

$$M_2 = 0.519, \quad \text{and} \quad p_{02}/p_{01} = 0.523.$$

There is no loss of stagnation pressure up to section 1, so $p_{01} = p_0$, which implies

$$p_{02} = 0.523 p_0 = 0.523(400) = 209.2 \text{ kPa}.$$

TABLE 15.2 One-Dimensional Normal-Shock Relations ($\gamma = 1.4$)

M_1	M_2	p_2/p_1	T_2/T_1	$(p_0)_2/(p_0)_1$	M_1	M_2	p_2/p_1	T_2/T_1	$(p_0)_2/(p_0)_1$
1	1	1	1	1	1.4	0.74	2.12	1.255	0.958
1.02	0.98	1.047	1.013	1	1.42	0.731	2.186	1.268	0.953
1.04	0.962	1.095	1.026	1	1.44	0.723	2.253	1.281	0.948
1.06	0.944	1.144	1.039	1	1.46	0.716	2.32	1.294	0.942
1.08	0.928	1.194	1.052	0.999	1.48	0.708	2.389	1.307	0.936
1.1	0.912	1.245	1.065	0.999	1.5	0.701	2.458	1.32	0.93
1.12	0.896	1.297	1.078	0.998	1.52	0.694	2.529	1.334	0.923
1.14	0.882	1.35	1.09	0.997	1.54	0.687	2.6	1.347	0.917
1.16	0.868	1.403	1.103	0.996	1.56	0.681	2.673	1.361	0.91
1.18	0.855	1.458	1.115	0.995	1.58	0.675	2.746	1.374	0.903
1.2	0.842	1.513	1.128	0.993	1.6	0.668	2.82	1.388	0.895
1.22	0.83	1.57	1.14	0.991	1.62	0.663	2.895	1.402	0.888
1.24	0.818	1.627	1.153	0.988	1.64	0.657	2.971	1.416	0.88
1.26	0.807	1.686	1.166	0.986	1.66	0.651	3.048	1.43	0.872
1.28	0.796	1.745	1.178	0.983	1.68	0.646	3.126	1.444	0.864
1.3	0.786	1.805	1.191	0.979	1.7	0.641	3.205	1.458	0.856
1.32	0.776	1.866	1.204	0.976	1.72	0.635	3.285	1.473	0.847
1.34	0.766	1.928	1.216	0.972	1.74	0.631	3.366	1.487	0.839
1.36	0.757	1.991	1.229	0.968	1.76	0.626	3.447	1.502	0.83
1.38	0.748	2.055	1.242	0.963	1.78	0.621	3.53	1.517	0.821

(*Continued*)

TABLE 15.2 One-Dimensional Normal-Shock Relations ($\gamma = 1.4$)—cont'd

M_1	M_2	p_2/p_1	T_2/T_1	$(p_0)_2/(p_0)_1$	M_1	M_2	p_2/p_1	T_2/T_1	$(p_0)_2/(p_0)_1$
1.8	0.617	3.613	1.532	0.813	2.42	0.521	6.666	2.06	0.532
1.82	0.612	3.698	1.547	0.804	2.44	0.519	6.779	2.079	0.523
1.84	0.608	3.783	1.562	0.795	2.46	0.517	6.894	2.098	0.515
1.86	0.604	3.869	1.577	0.786	2.48	0.515	7.009	2.118	0.507
1.88	0.6	3.957	1.592	0.777	2.5	0.513	7.125	2.138	0.499
1.9	0.596	4.045	1.608	0.767	2.52	0.511	7.242	2.157	0.491
1.92	0.592	4.134	1.624	0.758	2.54	0.509	7.36	2.177	0.483
1.94	0.588	4.224	1.639	0.749	2.56	0.507	7.479	2.198	0.475
1.96	0.584	4.315	1.655	0.74	2.58	0.506	7.599	2.218	0.468
1.98	0.581	4.407	1.671	0.73	2.6	0.504	7.72	2.238	0.46
2	0.577	4.5	1.688	0.721	2.62	0.502	7.842	2.26	0.453
2.02	0.574	4.594	1.704	0.711	2.64	0.5	7.965	2.28	0.445
2.04	0.571	4.689	1.72	0.702	2.66	0.499	8.088	2.301	0.438
2.06	0.567	4.784	1.737	0.693	2.68	0.497	8.213	2.322	0.431
2.08	0.564	4.881	1.754	0.683	2.7	0.496	8.338	2.343	0.424
2.1	0.561	4.978	1.77	0.674	2.72	0.494	8.465	2.364	0.417
2.12	0.558	5.077	1.787	0.665	2.74	0.493	8.592	2.386	0.41
2.14	0.555	5.176	1.805	0.656	2.76	0.491	8.721	2.407	0.403
2.16	0.553	5.277	1.822	0.646	2.78	0.49	8.85	2.429	0.396
2.18	0.55	5.378	1.837	0.637	2.8	0.488	8.98	2.451	0.389
2.2	0.547	5.48	1.857	0.628	2.82	0.487	9.111	2.473	0.383
2.22	0.544	5.583	1.875	0.619	2.84	0.485	9.243	2.496	0.376
2.24	0.542	5.687	1.892	0.61	2.86	0.484	9.376	2.518	0.37
2.26	0.539	5.792	1.91	0.601	2.88	0.483	9.51	2.541	0.364
2.28	0.537	5.898	1.929	0.592	2.9	0.481	9.645	2.563	0.358
2.3	0.534	6.005	1.947	0.583	2.92	0.48	9.781	2.586	0.352
2.32	0.532	6.113	1.965	0.575	2.94	0.479	9.918	2.609	0.346
2.34	0.53	6.222	1.984	0.566	2.96	0.478	10.055	2.632	0.34
2.36	0.527	6.331	2.003	0.557	2.98	0.476	10.194	2.656	0.334
2.38	0.525	6.442	2.021	0.549	3	0.475	10.333	2.679	0.328
2.4	0.523	6.553	2.04	0.54					

The value of A^* changes across a shock wave. The ratio A_2/A_2^* can be found from the *isentropic* table (Table 15.1) corresponding to a Mach number of $M_2 = 0.519$. (Note that A_2^* simply denotes the area that would be reached if the flow from state 2 were accelerated isentropically to sonic conditions.) For $M_2 = 0.519$, Table 15.1 gives:

$$A_2/A_2^* = 1.3, \text{ which leads to } A_2^* = A_2/1.3 = 0.5/1.3 = 0.3846 \text{ m}^2.$$

The flow from section 2 to section 3 is isentropic, during which A^* remains constant, so

$$A_3/A_3^* = A_3/A_2^* = 0.7/0.3846 = 1.82.$$

Now find the conditions at the nozzle exit from the isentropic table (Table 15.1). However, the value of $A/A^* = 1.82$ may be found either in the supersonic or the subsonic branch of the table. Since the flow downstream of a normal shock can only be subsonic, use the subsonic branch. For $A/A^* = 1.82$, Table 15.1 gives

$$T_3 = T_{03} = 0.977.$$

The stagnation temperature remains constant in an adiabatic process, so that $T_{03} = T_0$. Thus

$$T_3 = 0.977\ (800) = 782 \text{ K}.$$

15.8. EFFECTS OF FRICTION AND HEATING IN CONSTANT-AREA DUCTS

For steady one-dimensional compressible flow in a duct of constant cross-sectional area, the equations of mass, momentum, and energy conservation are:

$$\rho_1 u_1 = \rho_2 u_2,\ p_1 + \rho_1 u_1^2 = p_2 + \rho_2 u_2^2 + p_1 f, \quad \text{and} \quad h_1 + \frac{1}{2}u_1^2 + h_1 q = h_2 + \frac{1}{2}u_2^2, \tag{15.45}$$

where $f = F/(p_1 A)$ is a dimensionless friction parameter and $q = Q/h_1$ is a dimensionless heat transfer parameter. In terms of Mach number, for a perfect gas with constant specific heats, the momentum and energy equations become, respectively:

$$p_1(1 + \gamma M_1^2 - f) = p_2(1 + \gamma M_2^2), \quad \text{and} \quad h_1\left(1 + \frac{\gamma - 1}{2}M_1^2 + q\right) = h_2\left(1 + \frac{\gamma - 1}{2}M_2^2\right).$$

Using mass conservation, the thermal equation of state $p = \rho RT$, and the definition of the Mach number, all thermodynamic variables can be eliminated resulting in

$$\frac{M_2}{M_1} = \frac{1 + \gamma M_2^2}{1 + \gamma M_1^2 - f}\left[\frac{1 + \left((\gamma - 1)/2\right)M_1^2 + q}{1 + ((\gamma - 1)/2)M_2^2}\right]^{1/2}.$$

Bringing the unknown M_2 to the left-hand side and assuming q and f are specified along with M_1,

$$\frac{M_2^2\left(1+\frac{1}{2}(\gamma-1)M_2^2\right)}{\left(1+\gamma M_2^2\right)^2}=\frac{M_1^2\left(1+\frac{1}{2}(\gamma-1)M_1^2+q\right)}{\left(1+\gamma M_1^2-f\right)^2}\equiv A.$$

This is a biquadratic equation for M_2 with the solution:

$$M_2^2=\frac{-(1-2A\gamma)\pm[1-2A(\gamma+1)]^{1/2}}{(\gamma-1)-2A\gamma^2}. \tag{15.46}$$

Figures 15.15 and 15.16 are plots of M_2 versus M_1 from (15.46), first with f as a parameter and $q=0$ (Figure 15.15), and then with q as a parameter and $f=0$ (Figure 15.16). Generally, flow properties are known at the inlet station (1) and the flow properties at the outlet station (2) are

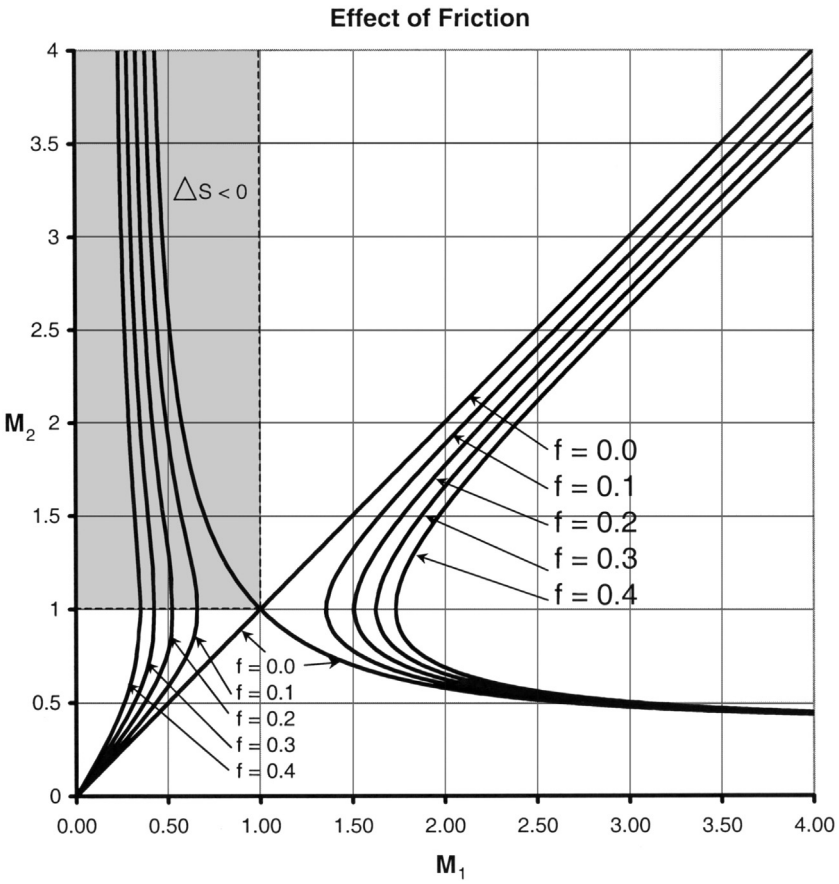

FIGURE 15.15 Flow in a constant-area duct with the dimensionless friction f as a parameter without heat exchange, $q=0$, at $\gamma=1.4$. The shaded region in the upper left is inaccessible because $\Delta S<0$. For any duct inlet value of M_1 the curves indicate possible outlet states. Interestingly, for $M_1<1$, all possible M_2 values are at a higher Mach number. For $M_1>1$, the two possible final states are both at lower Mach numbers.

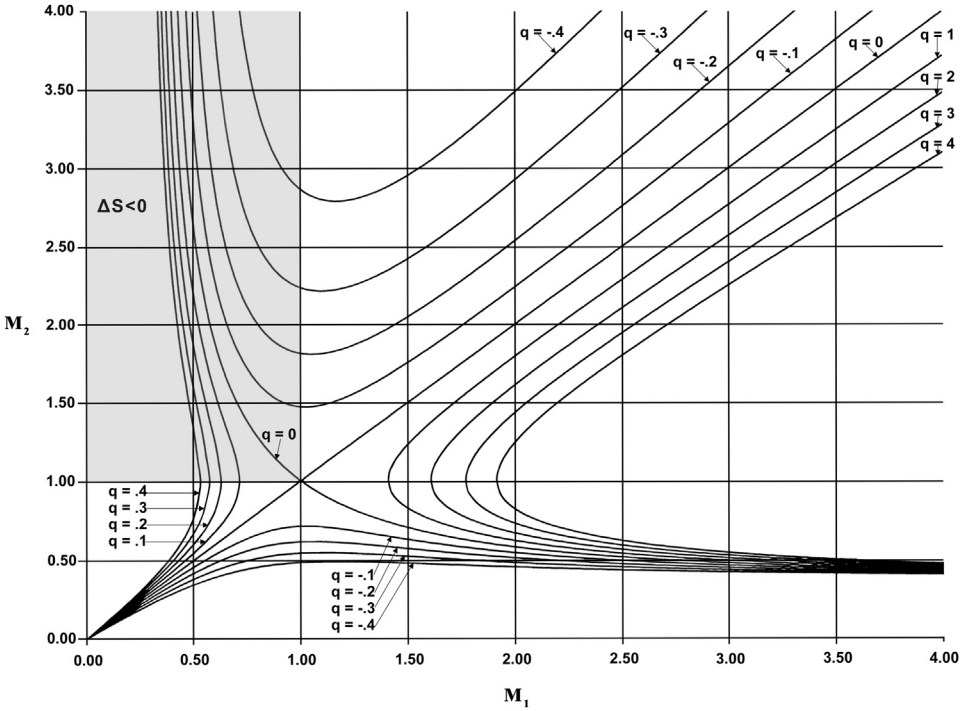

FIGURE 15.16 Flow in a constant-area duct with the dimensionless heat exchange q as a parameter without friction, $f = 0$, at $\gamma = 1.4$. The shaded region in the upper left is inaccessible because $\Delta S < 0$. Here, heat addition is seen to have much the same effect as friction.

sought. Here, the dimensionless friction f and heat transfer q are presumed to be specified. Thus, once M_2 is calculated from (15.45), all of the other properties may be obtained from the dimensionless formulation of the conservation laws above. When q and $f = 0$, two solutions are possible: the trivial solution $M_1 = M_2$ and the normal shock solution given in Section 15.6. We also showed that the upper left branch of the solution $M_2 > 1$ when $M_1 < 1$ is inaccessible because it violates the second law of thermodynamics, that is, it results in a spontaneous decrease of entropy.

Effect of Friction

Referring to the left branch of Figure 15.15, the solution indicates the surprising result that friction accelerates a subsonic flow leading to $M_2 > M_1$. This happens because friction causes the pressure, and therefore the density, to drop rapidly enough so that the fluid velocity must increase to maintain a constant mass flow. For this case of adiabatic flow with friction, the relevant equations for differential changes in pressure, velocity, and density in terms of the local Mach number $M = u/c$ are:

$$-\frac{dp}{p_1} = \frac{1 + (\gamma - 1)M^2}{1 - M^2} df, \quad \text{and} \quad \frac{du}{u} = -\frac{d\rho}{\rho} = \frac{p_1}{p} \frac{df}{1 - M^2}, \tag{15.47}$$

and these may be derived from (15.45) with $q = 0$ (Exercise 15.10). In particular since $df > 0$, (15.47) implies that dp/p_1 may have a large negative magnitude compared to df as M approaches unity from below. We will discuss in what follows what actually happens when there is no apparent solution for M_2. When M_1 is supersonic, two solutions are generally possible—one for which $1 < M_2 < M_1$ and the other where $M_2 < 1$. They are connected by a normal shock. Whether or not a shock occurs depends on the downstream pressure. There is also the possibility of M_1 insufficiently large or f too large so that no solution is indicated. We will discuss that in the following but note that the two solutions coalesce when $M_2 = 1$ and the flow is choked. At this condition the maximum mass flow is passed by the duct. In the case $1 < M_2 < M_1$, the flow is decelerated and the pressure, density, and temperature all increase in the downstream direction. The stagnation pressure is always decreased by friction as the entropy is increased. In summary, friction's net effect is to drive a compressible duct flow toward $M_2 = 1$ for any value of M_1.

Effect of Heat Transfer

The range of solutions is twice as rich in this case as q may take both signs while f must be positive. Figure 15.16 shows that for $q > 0$ solutions are similar in most respects to those with friction ($f > 0$). Heating accelerates a subsonic flow and lowers the pressure and density. However, heating generally increases the fluid temperature except in the limited range $1/\gamma < M_1^2 < 1$ in which the fluid temperature decreases with heat addition. The relevant equations for differential changes in temperature and flow speed in terms of the local Mach number $M = u/c$ are:

$$\frac{dT}{T_1} = \left(\frac{1 - \gamma M^2}{1 - M^2}\right) dq, \qquad \text{and} \qquad \frac{udu}{h_1} = \frac{(\gamma - 1)M^2}{1 - M^2} dq, \tag{15.48}$$

and these can be derived from (15.45) with $f = 0$ (Exercise 15.11). When $1/\gamma < M_1^2 < 1$, the energy from heat addition goes preferentially into increasing the velocity of the fluid. The supersonic branch $M_2 > 1$ when $M_1 < 1$ is inaccessible because those solutions violate the second law of thermodynamics. Again, as with f too large or M_1 too close to 1, there is a possibility no indicated solution when q is too large; this is discussed in what follows. When $M_1 > 1$, two solutions for M_2 are generally possible and they are connected by a normal shock. The shock is absent if the downstream pressure is low and present if the downstream pressure is high. Although $q > 0$ (and $f > 0$) does not always indicate a solution (if the flow has been choked), there will always be a solution for $q < 0$. Cooling a supersonic flow accelerates it, thus decreasing its pressure, temperature, and density. If no shock occurs, $M_2 > M_1$. Conversely, cooling a subsonic flow decelerates it so that the pressure and density increase. The temperature decreases when heat is removed from the flow except in the limited range $1/\gamma < M_1^2 < 1$ in which the heat removal decelerates the flow so rapidly that the temperature increases.

For high molecular-weight gases, near critical conditions (high pressure, low temperature), the gas dynamic relationships may be completely different from those developed here for perfect gases. Cramer and Fry (1993) found that nonperfect gases may support

expansion shocks, accelerated flow through "antithroats," and generally behave in unfamiliar ways.

Figures 15.15 and 15.16 show that friction or heat input in a constant-area duct both drive a compressible flow in the duct toward the sonic condition. For any given M_1, the maximum f or $q > 0$ that is permissible is the one for which $M = 1$ at the exit station. The flow is then said to be choked, and the mass flow rate through that duct cannot be increased without increasing p_1 or decreasing p_2. This is analogous to flow in a convergent duct. Imagine pouring liquid through a funnel from one container into another. There is a maximum volumetric flow rate that can be passed by the funnel, and beyond that flow rate, the funnel overflows. The same thing happens here. If f or q is too large, such that no (steady-state) solution is possible, there is an external adjustment that reduces the mass flow rate to that for which the exit speed is just sonic. For $M_1 < 1$ and $M_1 > 1$ the limiting curves for f and q indicating choked flow intersect $M_2 = 1$ at right angles. Qualitatively, the effect is the same as choking by area contraction.

15.9. PRESSURE WAVES IN PLANAR COMPRESSIBLE FLOW

To this point, the emphasis in this chapter has been on steady one-dimensional flows in which flow properties vary only in the direction of flow. This section presents compressible flow results for more than one spatial dimension. To get started, consider a point source emitting infinitesimal pressure (acoustic) disturbances in a still compressible fluid in which the speed of sound is c. If the point source is stationary, then the pressure-disturbance wave fronts are concentric spheres. Figure 15.17a shows the intersection of these wave fronts with a plane containing the source at times corresponding to integer multiples of Δt.

When the source propagates to the left at speed $U < c$, the wave-front diagram changes to look like Figure 15.17b, which shows four locations of the source separated by equal time intervals Δt, with point 4 being the present location of the source. At the first point, the source emitted a wave that has spherically expanded to a radius of $3c\Delta t$ in the time interval $3\Delta t$. During this time the source has moved to the fourth location, a distance of $3U\Delta t$ from the first point of wave-front emission. The figure also shows the locations of the wave fronts emitted while the source was at the second and third points. Here, the wave fronts do not intersect because $U < c$. As in the case of the stationary source, the wave fronts propagate vertically upward and downward, and horizontally upstream and downstream from the source. Thus, *a body moving at a subsonic speed influences the entire flow field*.

Now consider the case depicted in Figure 15.17c where the source moves supersonically, $U > c$. Here, the centers of the spherically expanding wave fronts are separated by more than $c\Delta t$, and no pressure disturbance propagates ahead of the source. Instead, the edges of the wave fronts form a conical tangent surface called the *Mach cone*. In planar two-dimensional flow, the tangent surface is in the form of a wedge, and the tangent lines are called *Mach lines*. An examination of the figure shows that the half-angle of the Mach cone (or wedge), called the *Mach angle* μ, is given by $\sin \mu = (c\Delta t)/(U\Delta t)$, so that

$$\sin \mu = 1/M. \tag{15.49}$$

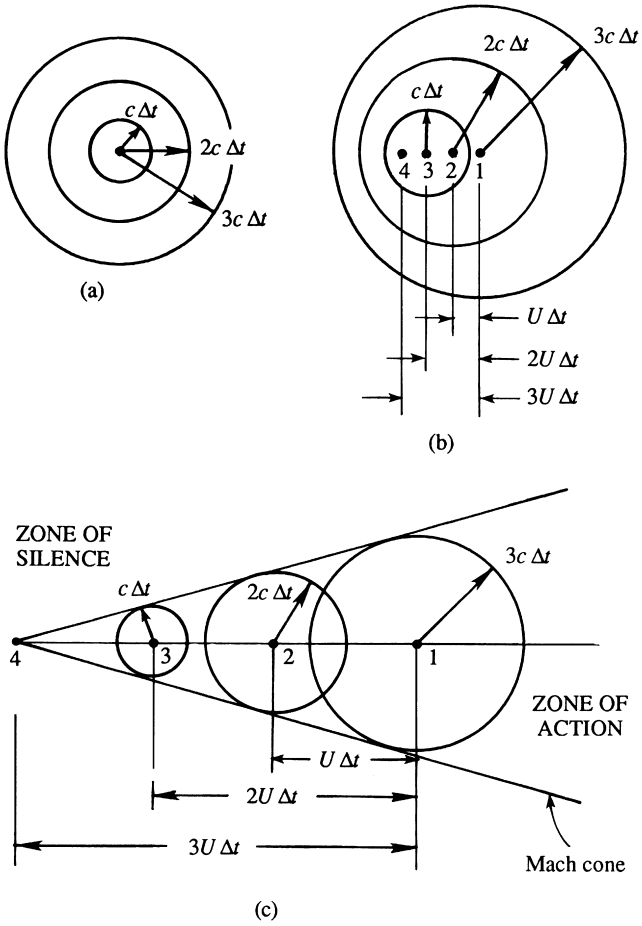

FIGURE 15.17 Wave fronts emitted by a point source in a still fluid when the source speed U is: (a) $U = 0$; (b) $U < c$; and (c) $U > c$. In each case the wave fronts are emitted at integer multiples of Δt. At subsonic source speeds, the wave fronts do not overlap and they spread ahead of the source. At supersonic source speeds, all the wave fronts lie behind the source within the Mach cone having a half-angle $\sin^{-1}(1/M)$.

The Mach cone becomes wider as M decreases and becomes a plane front (that is, $\mu = 90°$) when $M = 1$.

The point source considered here could be part of a solid body, which sends out pressure waves as it moves through the fluid. Moreover, after a simple Galilean transformation, Figure 15.17b and c apply equally well to a stationary point source with a compressible fluid moving past it at speed U. From Figure 15.17c it is clear that in a supersonic flow an observer outside the source's Mach cone would not detect or hear a pressure signal emitted by the source, hence this region is called the *zone of silence*. In contrast, the region inside the Mach cone is called the *zone of action*, within which the effects of the disturbance are felt. Thus, the sound of a supersonic aircraft passing overhead does not reach an observer on the ground

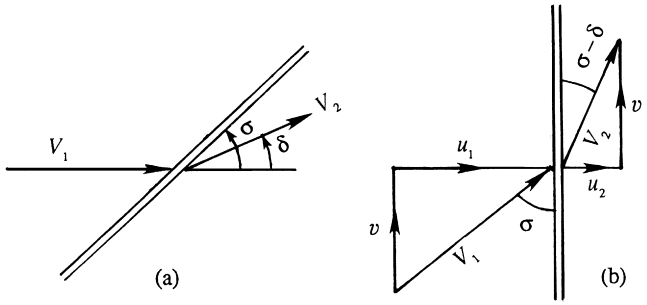

FIGURE 15.18 Two coordinate systems for an oblique shock wave. (a) Stream-aligned coordinates where the oblique shock wave lies at shock angle $= \sigma$ and produces a flow-deflection of angle $= \delta$. (b) Shock-normal coordinates which are preferred for analysis because an oblique shock wave is merely a normal shock with a superimposed shock-parallel velocity v.

until its Mach cone reaches the observer, and this arrival occurs *after* the aircraft has passed overhead.

At every point in a planar supersonic flow there are two Mach lines, oriented at $\pm\mu$ to the local direction of flow. Pressure disturbance information propagates along these lines, which are the *characteristics* of the governing differential equation. It can be shown that the nature of the governing differential equation is hyperbolic in a supersonic flow and elliptic in a subsonic flow.

When the pressure disturbances from the source are of finite amplitude, they may evolve into a shock wave that is not normal to the flow direction. Such *oblique* shock waves are commonly encountered in ballistics and supersonic flight, and differ from normal shock waves because they change the upstream flow velocity's magnitude *and* direction. A generic depiction of an oblique shock wave is provided in Figure 15.18 in two coordinate systems. Part a of this figure shows the stream-aligned coordinate system where the shock wave resides at an angle σ from the horizontal. Here the velocity upstream of the shock is horizontal with magnitude V_1, while the velocity downstream of the shock is deflected from the horizontal by an angle δ and has magnitude V_2. Part b of Figure 15.18 shows the same shock wave in a shock-aligned coordinate system where the shock wave is vertical, and the fluid velocities upstream and downstream of the shock are (u_1, v) and (u_2, v), respectively. Here v is parallel to the shock wave and is not influenced by it (see Exercise 15.18). Thus an oblique shock may be analyzed as a normal shock involving u_1 and u_2 to which a constant shock-parallel velocity v is added. Using the Cartesian coordinates in Figure 15.18b where the shock coincides with the vertical axis, the relationships between the various components and angles are:

$$(u_1, v) = \sqrt{u_1^2 + v^2}\,(\sin\sigma, \cos\sigma) = V_1(\sin\sigma, \cos\sigma),$$

and

$$(u_2, v) = \sqrt{u_2^2 + v^2}(\sin(\sigma - \delta), \cos(\sigma - \delta)) = V_2(\sin(\sigma - \delta), \cos(\sigma - \delta)).$$

The angle σ is called the *shock angle* or *wave angle* and δ is called the *deflection angle*. The normal Mach numbers upstream (1) and downstream (2) of the shock are:

$$M_{n1} = u_1/c_1 = M_1 \sin\sigma > 1,$$
$$M_{n2} = u_2/c_2 = M_2 \sin(\sigma - \delta) < 1.$$

Because $u_2 < u_1$, there is a sudden change of direction of flow across the shock and the flow is turned *toward* the shock by angle δ.

Superposition of the tangential velocity v does not affect the *static* properties, which are therefore the same as those for a normal shock. The expressions for the ratios p_2/p_1, ρ_2/ρ_1, T_2/T_1, and $(S_2 - S_1)/C_v$ are therefore those given by (15.39) and (15.41) through (15.43), if M_1 is replaced by $M_{n1} = M_1 \sin\sigma$. For example:

$$\frac{p_2}{p_1} = 1 + \frac{2\gamma}{\gamma+1}(M_1^2 \sin^2\sigma - 1), \tag{15.50}$$

$$\frac{\rho_2}{\rho_1} = \frac{(\gamma+1)M_1^2 \sin^2\sigma}{(\gamma-1)M_1^2 \sin^2\sigma + 2} = \frac{u_1}{u_2} = \frac{\tan\sigma}{\tan(\sigma - \delta)}. \tag{15.51}$$

Thus, the normal shock table, Table 15.2, is applicable to oblique shock waves if we use $M_1 \sin\sigma$ in place of M_1.

The relation between the upstream and downstream Mach numbers can be found from (15.40) by replacing M_1 by $M_1 \sin\sigma$ and M_2 by $M_2 \sin(\sigma - \delta)$. This gives

$$M_2^2 \sin^2(\sigma - \delta) = \frac{(\gamma-1)M_1^2 \sin^2\sigma + 2}{2\gamma M_1^2 \sin^2\sigma + 1 - \gamma}. \tag{15.52}$$

An important relation is that between the deflection angle δ and the shock angle σ for a given M_1, given in (15.51). Using the trigonometric identity for $\tan(\sigma - \delta)$, this becomes

$$\tan\delta = 2\cot\sigma \frac{M_1^2 \sin^2\sigma - 1}{M_1^2(\gamma + \cos 2\sigma) + 2}. \tag{15.53}$$

A plot of this relation is given in Figure 15.19. The curves represent δ versus σ for constant M_1. The value of M_2 varies along the curves, and the locus of points corresponding to $M_2 = 1$ is indicated. It is apparent that there is a maximum deflection angle δ_{max} for oblique shock solutions to be possible; for example, $\delta_{max} = 23^\circ$ for $M_1 = 2$. For a given M_1, δ becomes zero at $\sigma = \pi/2$ corresponding to a normal shock, and at $\sigma = \mu = \sin^{-1}(1/M_1)$ corresponding to the Mach angle. For a fixed M_1 and $\delta < \delta_{max}$, there are two possible solutions: a *weak shock* corresponding to a smaller σ and a *strong shock* corresponding to a larger σ. It is clear that the flow downstream of a strong shock is always subsonic; in contrast, the flow downstream of a weak shock is generally supersonic, except in a small range in which δ is slightly smaller than δ_{max}.

Oblique shock waves are commonly generated when a supersonic flow is forced to change direction to go around a structure where the flow area cross section is reduced.

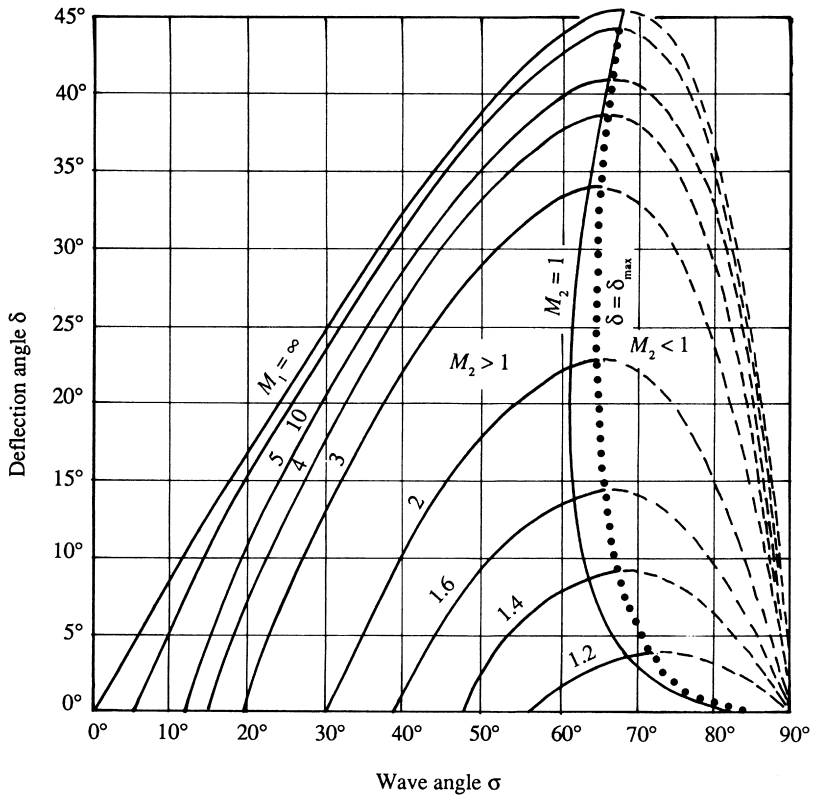

FIGURE 15.19 Plot of oblique shock solutions. The strong shock branch is indicated by dashed lines on the right, and the heavy dotted line indicates the maximum deflection angle δ_{max}. *(From Ames Research Staff, 1953, NACA Report 1135.)*

Two examples are shown in Figure 15.20 that show supersonic flow past a wedge of half-angle δ, or the flow past a compression bend where the wall turns into the flow by an angle δ. If M_1 and δ are known, then σ can be obtained from Figure 15.19, and M_{n2} (and therefore $M_2 = M_{n2}/\sin(\sigma - \delta)$) can be obtained from the shock table (Table 15.2). An attached shock wave, corresponding to the weak solution, forms at the nose of the wedge, such that the flow is parallel to the wedge after turning through an angle δ. The shock angle σ decreases to the Mach angle $\mu_1 = \sin^{-1}(1/M_1)$ as the deflection δ tends to

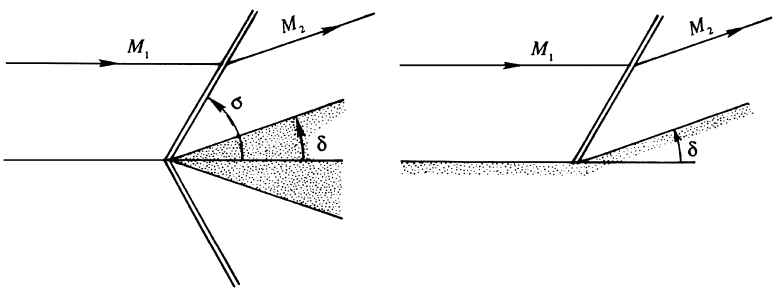

FIGURE 15.20 Two possible means for producing oblique shocks in a supersonic flow. In both cases a solid surface causes the flow to turn, and the flow area is reduced. The geometry shown in the right panel is sometimes called a *compression corner*.

zero. It is interesting that the corner velocity in a supersonic flow is finite. In contrast, the corner velocity in a subsonic (or incompressible) flow is either zero or infinite, depending on whether the wall shape is concave or convex. Moreover, the streamlines in Figure 15.20 are straight, and computation of the field is easy. By contrast, the streamlines in a subsonic flow are curved, and the computation of the flow field is not easy. The basic reason for this is that, in a supersonic flow, the disturbances do not propagate upstream of Mach lines or shock waves emanating from the disturbances, hence the flow field can be constructed step by step, *proceeding downstream*. In contrast, disturbances propagate both upstream and downstream in a subsonic flow so that all features in the entire flow field are related to each other.

As δ is increased beyond δ_{max}, attached oblique shocks are not possible, and a detached curved shock stands in front of the body (Figure 15.21). The central streamline goes through a normal shock and generates a subsonic flow in front of the wedge. The *strong* shock solution of Figure 15.19 therefore holds near the nose of the body. Farther out, the shock angle decreases, and the weak shock solution applies. If the wedge angle is not too large, then the curved detached shock in Figure 15.21 becomes an oblique attached shock as the Mach number is increased. In the case of a blunt-nosed body, however, the shock at the leading edge is always detached, although it moves closer to the body as the Mach number is increased.

We see that shock waves may exist in supersonic flows and their location and orientation adjust to satisfy boundary conditions. In external flows, such as those just described, the boundary condition is that streamlines at a solid surface must be tangent to that

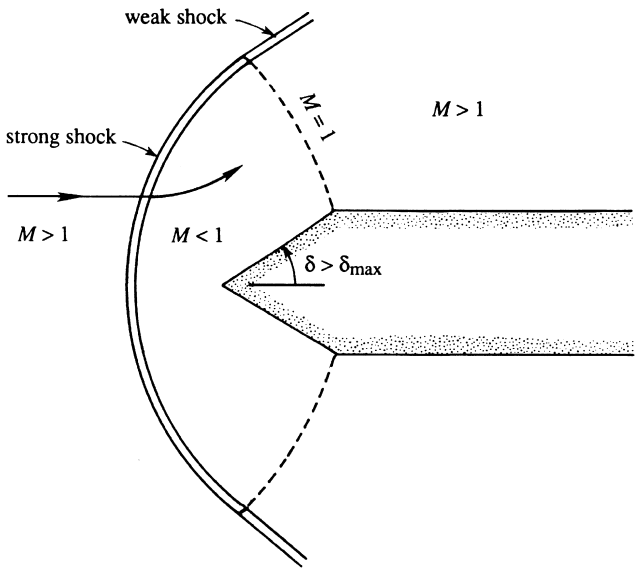

FIGURE 15.21 A detached shock wave. When the angle of the wedge shown in the left panel of Figure 15.20 is too great for an oblique shock, a curved shock wave will form that does not touch body. A portion of this detached shock wave will have the properties of a normal shock wave.

surface. In duct flows the boundary condition locating the shock is usually the downstream pressure.

From the foregoing analysis, it is clear that large-angle supersonic flow deflections should be avoided when designing efficient devices that produce minimal total pressure losses. Efficient devices tend to be slender and thin, and their performance may be analyzed using a weak oblique shock approximation that can be obtained from the results above in the limit of small flow deflection angle, $\delta \ll 1$. To obtain this expression, simplify (15.53) by noting that as $\delta \to 0$, the shock angle σ tends to the Mach angle $\mu_1 = \sin^{-1}(1/M_1)$. And, from (15.50) we note that $(p_2 - p_1)/p_1 \to 0$ as $M_1^2 \sin^2 \sigma - 1 \to 0$ (as $\sigma \to \mu$ and $\delta \to 0$). Then from (15.50) and (15.53):

$$\tan \delta = 2 \cot \sigma \frac{\gamma + 1}{2\gamma} \left(\frac{p_2 - p_1}{p_1} \right) \frac{1}{M_1^2(\gamma + 1 - 2 \sin^2 \sigma) + 2}. \tag{15.54}$$

As $\delta \to 0$, $\tan \delta \approx \delta$, $\cot \mu = \sqrt{M_1^2 - 1}$, $\sin \sigma \approx 1/M_1$, and

$$\frac{p_2 - p_1}{p_1} = \frac{\gamma M_1^2}{\sqrt{M_1^2 - 1}} \delta. \tag{15.55}$$

The interesting point is that the relation (15.55) is also applicable to weak *expansion* waves and not just weak compression waves. By this we mean that the pressure increase due to a small deflection of the wall toward the flow is the same as the pressure *decrease* due to a small deflection of the wall *away* from the flow. This extended range of validity of (15.55) occurs because the entropy change across a weak shock may be negligible even when the pressure change is appreciable (see (15.44b) and the related discussion). Thus, weak shock waves can be treated as isentropic or reversible. Relationships for a weak shock wave can therefore be applied to a weak expansion wave, except for some sign changes. In the final section of this chapter, (15.55) is used to estimate the lift and drag of a thin airfoil in supersonic flow.

When an initially horizontal supersonic flow follows a curving wall, the wall radiates compression and expansion waves into the flow that modulate the flow's direction and Mach number. When the wall is smoothly curved these compression and expansion waves follow Mach lines, inclined at an angle of $\mu = \sin^{-1}(1/M)$ to the *local* direction of flow (Figure 15.22). In this simple circumstance where there is no upper wall that radiates compression or expansion waves downward into the region of interest, the flow's orientation and Mach number are constant on each Mach line. In the case of compression, the Mach number decreases along the flow, so that the Mach angle increases. The Mach lines may therefore coalesce and form an oblique shock as in Figure 15.22a. In the case of a gradual expansion, the Mach number increases along the flow and the Mach lines diverge as in Figure 15.22b.

If the wall has a sharp deflection (a corner) away from the approaching stream, then the pattern of Figure 15.22b takes the form of Figure 15.23 where all the Mach lines originate from the corner. In this case, this portion of the flow where it expands and turns, and is not parallel to the wall upstream or downstream of the corner, is known as a *Prandtl-Meyer expansion fan*. The Mach number increases through the fan, with $M_2 > M_1$. The first Mach line

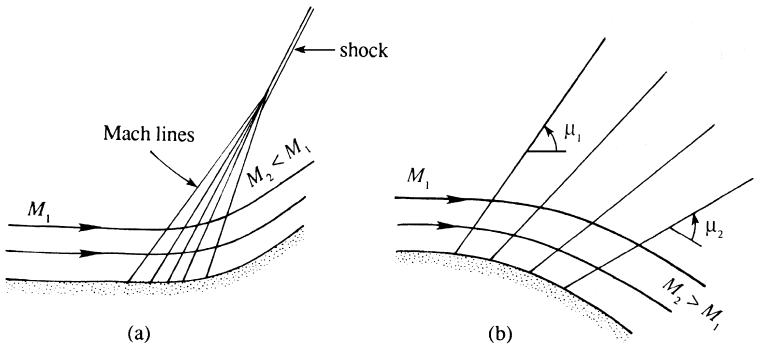

FIGURE 15.22 Gradual compression and expansion in supersonic flow. (a) A gradual compression corner like the one shown will eventually result in an oblique shock wave as the various Mach lines merge, each carrying a fraction of the overall compression. (b) A gradual expansion corner like the one shown produces Mach lines that diverge so the expansion becomes even more gradual farther from the wall.

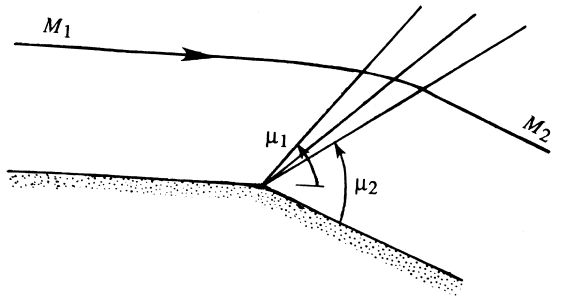

FIGURE 15.23 The Prandtl-Meyer expansion fan. This is the flow field developed by a sharp expansion corner. Here the flow area increases downstream of the corner so it accelerates a supersonic flow.

is inclined at an angle of μ_1 to the upstream wall direction, while the last Mach line is inclined at an angle of μ_2 to the downstream wall direction. The pressure falls gradually along any streamline through the fan. Along the wall, however, the pressure remains constant along the upstream wall, falls discontinuously at the corner, and then remains constant along the downstream wall. Figure 15.23 should be compared with Figure 15.20, in which the wall turns *inward* and generates an oblique shock wave. By contrast, the expansion in Figure 15.23 is gradual and isentropic away from the wall.

The flow through a Prandtl-Meyer expansion fan is calculated as follows. From Figure 15.18b, conservation of momentum tangential to the shock shows that the tangential velocity is unchanged, or:

$$V_1 \cos\sigma = V_2 \cos(\sigma - \delta) = V_2 (\cos\sigma \cos\delta + \sin\sigma \sin\delta).$$

We are concerned here with very small deflections, $\delta \to 0$ so $\sigma \to \mu$. Here, $\cos\delta \approx 1$, $\sin\delta \approx \delta$, $V_1 \approx V_2(1 + \delta \tan\sigma)$, so $(V_2 - V_1)/V_1 \approx -\delta \tan\sigma \approx -\delta/\sqrt{M_1^2 - 1}$, where $\tan\sigma \approx 1/\sqrt{M_1^2 - 1}$. Thus, the velocity change dV for an infinitesimal wall deflection $d\delta$ can be written as

$d\delta = -(dV/V)\sqrt{M^2-1}$ (first quadrant deflection). Because $V = Mc$, $dV/V = dM/M + dc/c$. With $c = \sqrt{\gamma RT}$ for a perfect gas, $dc/c = dT/2T$. Using (15.28) for adiabatic flow of a perfect gas, $dT/T = -(\gamma-1)M\,dM/[\,1+((\gamma-1)/2)M^2]$, then

$$d\delta = -\frac{\sqrt{M^2-1}}{M}\frac{dM}{1+\frac{1}{2}(\gamma-1)M^2}.$$

Integrating δ from 0 (radians) and M from 1 gives $\delta + \nu(M) = const.$, where

$$\nu(M) = \int_1^M \frac{\sqrt{M^2-1}}{1+\frac{1}{2}(\gamma-1)M^2}\frac{dM}{M} = \sqrt{\frac{\gamma+1}{\gamma-1}}\tan^{-1}\sqrt{\frac{\gamma-1}{\gamma+1}(M^2-1)} - \tan^{-1}\sqrt{M^2-1} \quad (15.56)$$

is called the *Prandtl-Meyer function*. The sign of $\sqrt{M^2-1}$ originates from the identification of $\tan\sigma = \tan\mu = 1/\sqrt{M^2-1}$ for a first quadrant deflection (upper half-plane). For a fourth quadrant deflection (lower half-plane), $\tan\mu = -1/\sqrt{M^2-1}$. For example, for Figure 15.22a or b with δ_1, δ_2, and M_1 given, we would write

$$\delta_1 + \nu(M_1) = \delta_2 + \nu(M_2), \text{ and then } \nu(M_2) = \delta_1 - \delta_2 + \nu(M_1)$$

would determine M_2. In Figure 15.22a, $\delta_1 - \delta_2 < 0$, so $v_2 < v_1$ and $M_2 < M_1$. In Figure 15.22b, $\delta_1 - \delta_2 > 0$, so $v_2 > v_1$ and $M_2 > M_1$.

15.10. THIN AIRFOIL THEORY IN SUPERSONIC FLOW

Simple expressions can be derived for the lift and drag coefficients of an airfoil in supersonic flow if the thickness and angle of attack are small. Under these circumstances the pressure disturbances caused by the airfoil are small, and the total flow can be built up by superposition of small disturbances emanating from points on the body. Such a linearized theory of lift and drag was developed by Ackeret. Because all flow inclinations are small, we can use the relation (15.55) to calculate the pressure changes due to a change in flow direction. We can write this relation as

$$\frac{p-p_\infty}{p_\infty} = \frac{\gamma M_\infty^2\,\delta}{\sqrt{M_\infty^2-1}}, \quad (15.57)$$

where p_∞ and M_∞ refer to the properties of the free stream, and p is the pressure at a point where the flow is inclined at an angle δ to the free-stream direction. The sign of δ in (15.57) determines the sign of $(p-p_\infty)$.

To see how the lift and drag of a thin body in a supersonic stream can be estimated, consider a flat plate inclined at a small angle α to a horizontal stream (Figure 15.24). At the leading edge there is a weak expansion fan above the top surface and a weak oblique shock below the bottom surface. The streamlines ahead of these waves are straight. The streamlines above the plate turn through an angle α by expanding through an expansion fan, downstream of which they become parallel to the plate with a pressure $p_2 < p_\infty$. The upper streamlines

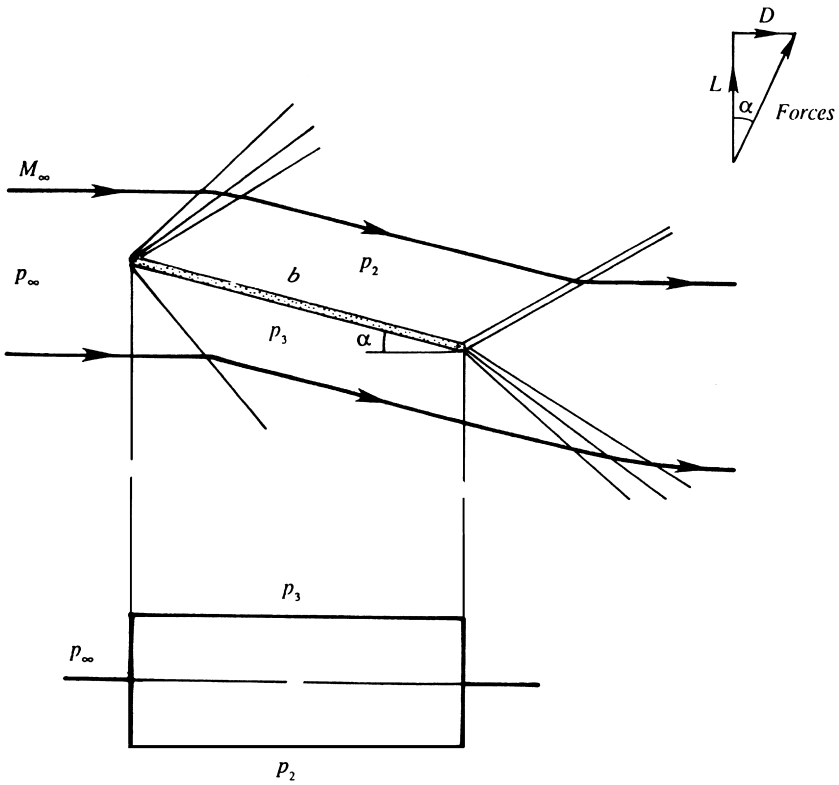

FIGURE 15.24 Inclined flat plate in a supersonic stream as a simple illustration of supersonic aerodynamics. The upper panel shows the flow pattern and the lower panel shows the pressure distribution on the suction and pressure sides of the simple foil. Here, an ideal compressible flow analysis does predict a drag component, unlike an equivalent ideal incompressible flow.

then turn sharply across an oblique shock emanating from the trailing edge, becoming parallel to the free stream once again. Opposite features occur for the streamlines below the plate where the flow first undergoes compression across an oblique shock coming from the leading edge, which results in a pressure $p_3 > p_\infty$. It is, however, not important to distinguish between shock and expansion waves in Figure 15.24, because the linearized theory treats them the same way, except for the sign of the pressure changes they produce.

The pressures above and below the plate can be found from (15.47), giving:

$$\frac{p_2 - p_\infty}{p_\infty} = -\frac{\gamma M_\infty^2 \alpha}{\sqrt{M_\infty^2 - 1}}, \quad \text{and} \quad \frac{p_3 - p_\infty}{p_\infty} = \frac{\gamma M_\infty^2 \alpha}{\sqrt{M_\infty^2 - 1}}.$$

The pressure difference across the plate is therefore

$$\frac{p_3 - p_2}{p_\infty} = \frac{2\alpha\gamma M_\infty^2}{\sqrt{M_\infty^2 - 1}}.$$

If b is the chord length, then the lift L and drag D forces per unit span are:

$$L = (p_3 - p_2)\, b \cos\alpha \cong \frac{2\alpha\gamma M_\infty^2 p_\infty b}{\sqrt{M_\infty^2 - 1}}, \quad \text{and} \quad D = (p_3 - p_2)\, b \sin\alpha \cong \frac{2\alpha^2\gamma M_\infty^2 p_\infty b}{\sqrt{M_\infty^2 - 1}}. \tag{15.58}$$

Using the relationship $\rho U^2 = \gamma p M^2$, the lift and drag coefficients are:

$$C_L = \frac{L}{(1/2)\rho_\infty U_\infty^2 b} \cong \frac{4\alpha}{\sqrt{M_\infty^2 - 1}}, \quad \text{and} \quad C_D = \frac{D}{(1/2)\rho_\infty U_\infty^2 b} \cong \frac{4\alpha^2}{\sqrt{M_\infty^2 - 1}}. \tag{15.59}$$

These expressions do not hold at transonic speeds $M_\infty \to 1$, when the process of linearization used here breaks down. The expression for the lift coefficient should be compared to the incompressible expression $C_L = 2\pi\alpha$ derived in the preceding chapter. Note that the flow in Figure 15.24 does have a circulation because the velocities at the upper and lower surfaces are parallel but have different magnitudes. However, in a supersonic flow it is not necessary to invoke the Kutta condition (discussed in the preceding chapter) to determine the magnitude of the circulation. The flow in Figure 15.24 does leave the trailing edge smoothly.

The drag in (15.59) is the *wave drag* experienced by a body in a supersonic stream, and exists even in an inviscid flow. The d'Alembert paradox therefore does not apply in a supersonic flow. The supersonic wave drag is analogous to the gravity wave drag experienced by a ship moving at a speed greater than the velocity of surface gravity waves, in which a system of bow waves is carried with the ship. The magnitude of the supersonic wave drag is independent of the value of the viscosity, although the energy spent in overcoming this drag is finally dissipated through viscous effects within the shock waves. In addition to the wave drag, additional drags due to viscous and finite-span effects, considered in the preceding chapter, act on a real wing.

In this connection, it is worth noting the difference between the airfoil shapes used in subsonic and supersonic airplanes. Low-speed airfoils have a streamlined shape, with a rounded nose and a sharp trailing edge. These features are not helpful in supersonic airfoils. The most effective way to reduce the drag of a supersonic airfoil is to reduce its thickness. Supersonic wings are characteristically thin and have sharp leading edges.

EXERCISES

15.1. The field equation for one-dimensional acoustic pressure fluctuations in an ideal compressible fluid is (15.13).

a) Change the independent variables x and t to $\xi = x - ct$ and $\zeta = x + ct$ to simplify (15.13) to $\dfrac{\partial^2 p'}{\partial\xi\partial\zeta} = 0$.

b) Use the simplified equation in part a) to find the general solution to the original field equation: $p'(x,t) = f(x - ct) + g(x + ct)$ where f and g are undetermined functions.

c) When the initial conditions are: $p' = F(x)$ and $\partial p'/\partial t = G(x)$ at $t = 0$, show that:

$$f(x) = \frac{1}{2}\left[F(x) - \frac{1}{c}\int_0^x G(\varkappa)d\varkappa\right], \quad \text{and} \quad g(x) = \frac{1}{2}\left[F(x) + \frac{1}{c}\int_0^x G(\varkappa)d\varkappa\right],$$

where $\varkappa$ is just an integration variable.

15.2. Starting from (15.15) use (15.14) to prove (15.16).

15.3. Consider two approaches to determining the upper Mach number limit for incompressible flow.

a) First consider pressure errors in the simplest possible steady-flow Bernoulli equation. Expand (15.29) for small Mach number to determine the next term in the expansion: $p_0 = p + (1/2)\rho u^2 + \ldots$ and determine the Mach number at which this next term is 5% of p when $\gamma = 1.4$.

b) Second consider changes to the density. Expand (15.30) for small Mach number and determine the Mach number at which the density ratio ρ_0/ρ differs from unity by 5% when $\gamma = 1.4$.

c) Which criterion is correct? Explain why the criteria for incompressibility determined in parts a) and b) differ, and reconcile them if you can.

15.4. The critical area A^* of a duct flow was defined in Section 15.4. Show that the relation between A^* and the actual area A at a section, where the Mach number equals M, is that given by (15.31). This relation was not proved in the text. [*Hint*: Write

$$\frac{A}{A^*} = \frac{\rho^* c^*}{\rho u} = \frac{\rho^*}{\rho_0}\frac{\rho_0}{\rho}\frac{c^*}{c}\frac{c}{u} = \frac{\rho^*}{\rho_0}\frac{\rho_0}{\rho}\sqrt{\frac{T^*}{T_0}\frac{T_0}{T}}\frac{1}{M}.$$

Then use the other relations given in Section 15.4.]

15.5. The entropy change across a normal shock is given by (15.43). Show that this reduces to expressions (15.44a and b) for weak shocks. [*Hint*: Let $M_1^2 - 1 \ll 1$. Write the terms within the two sets of brackets in equation (15.43) in the form $[1 + \varepsilon_1]\,[1 + \varepsilon_2]^\gamma$, where ε_1 and ε_2 are small quantities. Then use series expansion $\ln(1 + \varepsilon) = \varepsilon - \varepsilon^2/2 + \varepsilon^3/3 + \ldots$. This gives equation (15.44) times a function of M_1 in which we can set $M_1 = 1$.]

15.6. Show that the maximum velocity generated from a reservoir in which the stagnation temperature equals T_0 is $u_{\max} = \sqrt{2C_pT_0}$. What are the corresponding values of T and M?

15.7. In an adiabatic flow of air through a duct, the conditions at two points are $u_1 = 250$ m/s, $T_1 = 300$ K, $p_1 = 200$ kPa, $u_2 = 300$ m/s, and $p_2 = 150$ kPa. Show that the loss of stagnation pressure is nearly 34.2 kPa. What is the entropy increase?

15.8. A shock wave generated by an explosion propagates through a still atmosphere. If the pressure downstream of the shock wave is 700 kPa, estimate the shock speed and the flow velocity downstream of the shock.

15.9. Using dimensional analysis, G. I. Taylor deduced that the radius $R(t)$ of the blast wave from a large explosion would be proportional to $(E/\rho_1)^{1/5}t^{2/5}$ where E is the explosive energy, ρ_1 is the quiescent air density ahead of the blast wave, and t is the time since the blast (see Example 1.4). The goal of this problem is to (approximately) determine the constant of proportionality assuming perfect-gas thermodynamics.

a) For the strong shock limit where $M_1^2 \gg 1$, show:

$$\frac{\rho_2}{\rho_1} \cong \frac{\gamma+1}{\gamma-1}, \quad \frac{T_2}{T_1} \cong \frac{\gamma-1}{\gamma+1}\frac{p_2}{p_1}, \quad \text{and} \quad u_1 = M_1 c_1 \cong \sqrt{\frac{\gamma+1}{2}\frac{p_2}{\rho_1}}.$$

b) For a perfect gas with internal energy per unit mass e, the internal energy per unit volume is ρe. For a hemispherical blast wave, the volume inside the blast wave will be $(2/3)\pi R^3$. Thus, set $\rho_2 e_2 = E/(2/3)\pi R^3$, determine p_2, set $u_1 = dR/dt$, and integrate the resulting first-order differential equation to show that $R(t) = K(E/\rho_1)^{1/5} t^{2/5}$ when $R(0) = 0$ and K is a constant that depends on "γ".

c) Evaluate K for $\gamma = 1.4$. A similarity solution of the non-linear gas-dynamic equations in spherical coordinates produces $K = 1.033$ for $\gamma = 1.4$ (see Thompson 1972, p. 501). What is the percentage error in this exercise's approximate analysis?

15.10. Starting from the set (15.45) with $q = 0$, derive (15.47) by letting station (2) be a differential distance downstream of station (1).

15.11. Starting from the set (15.45) with $f = 0$, derive (15.48) by letting station (2) be a differential distance downstream of station (1).

15.12. A wedge has a half-angle of 50°. Moving through air, can it ever have an attached shock? What if the half-angle were 40°? [*Hint*: The argument is based entirely on Figure 15.19.]

15.13. Air at standard atmospheric conditions is flowing over a surface at a Mach number of $M_1 = 2$. At a downstream location, the surface takes a sharp inward turn by an angle of 20°. Find the wave angle σ and the downstream Mach number. Repeat the calculation by using the weak shock assumption and determine its accuracy by comparison with the first method.

15.14. A flat plate is inclined at 10° to an airstream moving at $M_\infty = 2$. If the chord length is $b = 3$ m, find the lift and wave drag per unit span.

15.15. A perfect gas is stored in a large tank at the conditions specified by p_0, T_0. Calculate the maximum mass flow rate that can exhaust through a duct of cross-sectional area A. Assume that A is small enough that during the time of interest p_0 and T_0 do not change significantly and that the flow is adiabatic.

15.16. For flow of a perfect gas entering a constant area duct at Mach number M_1, calculate the maximum admissible values of f, q for the same mass flow rate. Case (a) $f = 0$; case (b) $q = 0$.

15.17. Using thin airfoil theory calculate the lift and drag on the airfoil shape given by $y_u = t \sin(\pi x/c)$ for the upper surface and $y_l = 0$ for the lower surface. Assume a supersonic stream parallel to the x-axis. The thickness ratio $t/c \ll 1$.

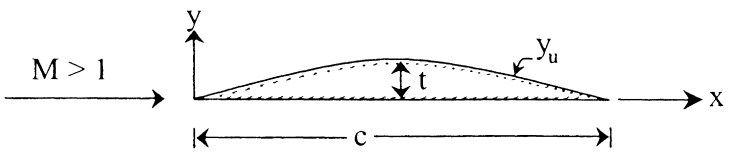

15.18. Write momentum conservation for the volume of the small cylindrical control volume shown in Figure 4.18 where the interface is a shock with flow from side 1 to side 2. Let the two end faces approach each other as the shock thickness → 0 and assume viscous stresses may be neglected on these end faces (outside the structure). Show that the $\boldsymbol{n}$ component of momentum conservation yields (15.36) and the $\boldsymbol{t}$ component gives $\boldsymbol{u} \cdot \boldsymbol{t}$ is conserved or v is continuous across the shock.

Literature Cited

Ames Research Staff (1953). NACA Report 1135: Equations, Tables, and Charts for Compressible Flow.
Becker, R. (1922). Stosswelle und Detonation. *Z. Physik, 8*, 321–362.
Cohen, I. M., & Moraff, C. A. (1971). Viscous inner structure of zero Prandtl number shocks. *Phys. Fluids, 14*, 1279–1280.
Cramer, M. S., & Fry, R. N. (1993). Nozzle flows of dense gases. *The Physics of Fluids A, 5*, 1246–1259.
Fergason, S. H., Ho, T. L., Argrow, B. M., & Emanuel, G. (2001). Theory for producing a single-phase rarefaction shock wave in a shock tube. *Journal of Fluid Mechanics, 445*, 37–54.
Hayes, W. D. (1958). The basic theory of gasdynamic discontinuities, Sect. D of *Fundamentals of Gasdynamics*. In H. W. Emmons (Ed.), Vol. III of *High Speed Aerodynamics and Jet Propulsion*. Princeton, NJ: Princeton University Press.
Liepmann, H. W., & Roshko, A. (1957). *Elements of Gas Dynamics*. New York: Wiley.
Pierce, A. D. (1989). *Acoustics*. New York: Acoustical Society of America.
Shapiro, A. H. (1953). *The Dynamics and Thermodynamics of Compressible Fluid Flow*, 2 volumes. New York: Ronald.
Thompson, P. A. (1972). *Compressible Fluid Dynamics*. New York: McGraw-Hill.
von Karman, T. (1954). *Aerodynamics*. New York: McGraw-Hill.

Supplemental Reading

Courant, R., & Friedrichs, K. O. (1977). *Supersonic Flow and Shock Waves*. New York: Springer-Verlag.
Yahya, S. M. (1982). *Fundamentals of Compressible Flow*. New Delhi: Wiley Eastern.